AMERICAN SOCIETY FOR MICROBIOLOGY | Applied and Environmental Microbiology®

ENVIRONMENTAL MICROBIOLOGY

ABC Transporter DerAB of *Lactobacillus casei* Mediates Resistance against Insect-Derived Defensins

Ainhoa Revilla-Guarinos,[a] Qian Zhang,[a] Christoph Loderer,[a] Cristina Alcántara,[b] Ariane Müller,[c] Mohammad Rahnamaeian,[d] Andreas Vilcinskas,[d,e] Susanne Gebhard,[f] Manuel Zúñiga,[b] Thorsten Mascher[a]

[a]Institut für Mikrobiologie, Technische Universität Dresden, Dresden, Germany
[b]Instituto de Agroquímica y Tecnología de Alimentos (IATA-CSIC), Valencia, Spain
[c]Institut für Zoologie, Technische Universität Dresden, Dresden, Germany
[d]Fraunhofer Institute for Molecular Biology and Applied Ecology, Department of Bioresources, Giessen, Germany
[e]Institute for Insect Biotechnology, Justus Liebig University Giessen, Giessen, Germany
[f]Department of Biology and Biochemistry, Milner Centre for Evolution, University of Bath, United Kingdom

ABSTRACT Bce-like systems mediate resistance against antimicrobial peptides in *Firmicutes* bacteria. *Lactobacillus casei* BL23 encodes an "orphan" ABC transporter that, based on homology to BceAB-like systems, was proposed to contribute to antimicrobial peptide resistance. A mutant lacking the permease subunit was tested for sensitivity against a collection of peptides derived from bacteria, fungi, insects, and humans. Our results show that the transporter specifically conferred resistance against insect-derived cysteine-stabilized $\alpha\beta$ defensins, and it was therefore renamed DerAB for defensin resistance ABC transporter. Surprisingly, cells lacking DerAB showed a marked increase in resistance against the lantibiotic nisin. This could be explained by significantly increased expression of the antimicrobial peptide resistance determinants regulated by the Bce-like systems PsdRSAB (formerly module 09) and ApsRSAB (formerly module 12). Bacterial two-hybrid studies in *Escherichia coli* showed that DerB could interact with proteins of the sensory complex in the Psd resistance system. We therefore propose that interaction of DerAB with this complex in the cell creates signaling interference and reduces the cell's potential to mount an effective nisin resistance response. In the absence of DerB, this negative interference is relieved, leading to the observed hyperactivation of the Psd module and thus increased resistance to nisin. Our results unravel the function of a previously uncharacterized Bce-like orphan resistance transporter with pleiotropic biological effects on the cell.

IMPORTANCE Antimicrobial peptides (AMPs) play an important role in suppressing the growth of microorganisms. They can be produced by bacteria themselves—to inhibit competitors—but are also widely distributed in higher eukaryotes, including insects and mammals, where they form an important component of innate immunity. In low-GC-content Gram-positive bacteria, BceAB-like transporters play a crucial role in AMP resistance but have so far been primarily associated with interbacterial competition. Here, we show that the orphan transporter DerAB from the lactic acid bacterium *Lactobacillus casei* is crucial for high-level resistance against insect-derived AMPs. It therefore represents an important mechanism for interkingdom defense. Furthermore, our results support a signaling interference from DerAB on the PsdRSAB module that might prevent the activation of a full nisin response. The Bce modules from *L. casei* BL23 illustrate a biological paradox in which the intrinsic nisin detoxification potential only arises in the absence of a defensin-specific ABC transporter.

KEYWORDS ABC transporters, antimicrobial peptide resistance, cell envelope stress response, defensins, nisin, two-component system

Citation Revilla-Guarinos A, Zhang Q, Loderer C, Alcántara C, Müller A, Rahnamaeian M, Vilcinskas A, Gebhard S, Zúñiga M, Mascher T. 2020. ABC transporter DerAB of *Lactobacillus casei* mediates resistance against insect-derived defensins. Appl Environ Microbiol 86:e00818-20. https://doi.org/10.1128/AEM.00818-20.

Editor Harold L. Drake, University of Bayreuth

Address correspondence to Ainhoa Revilla-Guarinos, ainhoa.revilla-guarinos@tu-dresden.de, or Thorsten Mascher, thorsten.mascher@tu-dresden.de.

Received 7 April 2020
Accepted 9 May 2020
Accepted manuscript posted online 15 May 2020
Published 2 July 2020

Antimicrobial peptides (AMPs) are found in all domains of life and constitute an important aspect of the natural immune response of many organisms (1, 2). AMPs are considered an alternative to classical antibiotics, since the development of resistance has occurred to a lesser extent (3, 4). One prominent mechanism of action of AMPs is binding to lipid II, which leads to the inhibition of bacterial cell wall biosynthesis, often followed by pore formation with the concomitant release of cell metabolites and the loss of membrane potential (5–7). Most AMPs are structurally very diverse, amphipathic molecules composed of 5 to 60 amino acids with a net positive charge (http://aps.unmc.edu/AP/main.php) (8). Nisin and subtilin are elongated, flexible, positively charged type A lantibiotics, while mersacidin is a more globular and rigid type B lantibiotic with a net negative charge (9). Insect AMPs such as cecropins have an α-helical structure, while defensins have a cysteine-stabilized structure consisting of an N-terminal loop followed by an α-helix and an antiparallel β-sheet (CS$\alpha\beta$), which are linked by disulfide bridges (10, 11).

Since AMPs represent common threats in microbial habitats, bacteria have developed a wide range of different AMP resistance mechanisms (3, 12). General or nonspecific resistance is conferred by changing the bacterial surface properties. The *dlt* (D-alanyl-lipoteichoic acid) operon mediates the D-alanylation of lipoteichoic acid (LTA) and wall teichoic acid (WTA) (13, 14), while expression of *mprF* (multiple peptide resistance factor) modifies anionic phospholipids of the membrane with L-lysine or L-alanine (15, 16). In both cases, the resulting decrease in the net negative charge of the bacterial envelope reduces the access of cationic AMPs to their surface targets, thereby conferring resistance. Unlike with this general AMP resistance, ABC transporters constitute compound-specific resistance determinants for AMP detoxification by actively removing the peptides from their site of action (17).

Bce-like systems, named after BceAB from *Bacillus subtilis*, represent a unique type of AMP-detoxifying ABC transporters (18, 19). They most likely consist of two nucleotide-binding domain (NBD) subunits (ATPases) and a membrane-spanning domain (MSD) subunit (permease) (20) and are functionally and genetically associated with BceRS-like two-component systems (TCS) (21, 22). The transporter confers resistance by a target protection mechanism, in which constant removal of the AMP from its cellular target keeps sufficient amounts of lipid II cycle intermediates available to ensure continued cell wall synthesis (23, 24). The transporter works in a sensory complex with the histidine kinase (HK) BceS (20). Signaling within this complex is activated in response to transport activity (25), which is achieved by the transporter directly controlling the conformational state of the HK (26). Upon activation, BceS then phosphorylates BceR, its cognate response regulator (RR), which in turn induces the expression of *bceAB* and sometimes that of additional target genes, which ensures antibiotic resistance. Since this detoxification process also removes the antibiotic from its site of detection (i.e., the transport activity of the resistance transporter decreases), Bce-dependent signaling is gradually switched off again (25, 26).

So-called "dual-function" BceAB-like transporters are required for both sensing the presence of the AMPs (input) and their detoxification (output). However, a division of labor between Bce-like transporters can be found in some systems. In these systems, a specialized "sensing transporter" perceives the signal and passes this information on to its cognate TCS, which in turn leads to the expression of a second "resistance transporter" that removes the AMP from the cell surface (12, 27).

So far, the specificity of BceAB-like transporters has not been correlated with any particular characteristic feature of the AMPs, such as structure, origin, modification, or mechanism of action (17, 21, 28). Some transporters can confer resistance against structurally very different AMPs, while at the same time being able to distinguish between very similar compounds. For example, the Psd system of *Bacillus subtilis* responds to actagardine and enduracidin but not to mersacidin or ramoplanin (29). Intriguingly, BceAB-like transporters can even be induced by AMPs against which they do not mediate any resistance; e.g., PsdAB is induced by actagardine but does not confer resistance against it (29). This behavior indicates that sensing and removal of

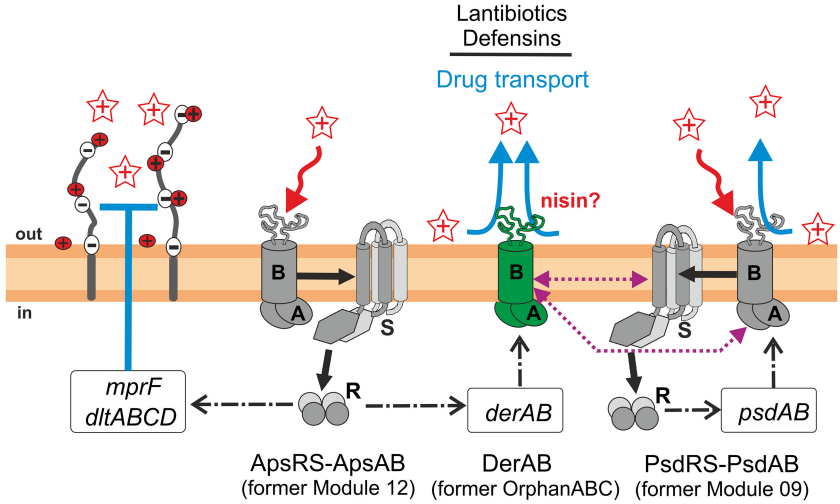

FIG 1 Different layers of resistance against AMPs in *L. casei* BL23. ApsRSAB is a sensory module that regulates different layers of resistance against numerous AMPs. The primary layer of AMP resistance is mediated by DerAB (drug transport), and the secondary layer of resistance is mediated by the Dlt system and MprF protein (drug repulsion). Resistance mediated by DerAB is specific for defensins and—to a lesser degree—lantibiotics (see the text for details). PsdRSAB is a dual-function module involved in the sensing and transport of various AMPs. AMPs are depicted as red positively charged starts. S, histidine kinase; R, response regulator; B, permease; A, ATPase. Homodimers of histidine kinases (HKs) and response regulators (RRs) are indicated. ABC transporters are composed of a permease subunit and two ATPase domains (20). Signaling between the permeases and the HKs and between the HKs and the RRs is indicated by black solid arrows. Gene activation and the increased production of the transporters is indicated by black dash-dot arrows. Wave-shaped, downward red arrows indicate sensing of AMPs; blue upward-facing arrows indicate transport and detoxification. B2H protein-protein interactions of DerB with PsdRSAB are indicated with purple dotted lines. Lipoteichoic acids are indicated with gray negatively charged lines; D-alanylation of teichoic acids and L-lysinilation of membrane phospholipids is indicated with positive red-filled circles; AMP charge repulsion is indicated with a barred, upward-facing blue line.

AMPs are two separable functions of BceAB-like transporters, an assumption that has been genetically verified for BceAB of *B. subtilis* (30).

L. casei BL23 encodes 17 TCSs (31), two of which, TCS09 and TCS12, are homologous to BceRS from *B. subtilis*. Both systems are genomically and functionally associated with the BceAB-like transporters ABC09 and ABC12 and constitute functional Bce-like units that were initially referred to as module 09 and module 12 (32). Module 09 is a standalone detoxification system, in which ABC09 is a dual-function transporter and *abc09* is the only known target operon of RR09. TCS09 responds to nisin via ABC09 and induces the expression of the transporter, which then confers nisin resistance (Fig. 1). Module 09 additionally confers resistance against bacitracin, plectasin, and subtilin (32). Because its inducer/substrate spectrum and regulatory behavior resemble those of PsdRSAB from *B. subtilis* (29), we renamed module 09 PsdRSAB, for peptide antibiotic sensing and detoxification. For module 12, ABC12 is a sensing transporter that is not involved in the detoxification process. In response to nisin, the cognate RR12 instead induces the expression of a larger regulon that includes the *dlt* operon, the *mprF* gene, and an operon encoding an orphan BceAB-like ABC transporter of unknown function (Fig. 1). Module 12 deletion mutants are sensitive to bacitracin, nisin, subtilin, mersacidin, plectasin, and vancomycin, mainly due to the impaired functionality of the Dlt system, which also renders these mutants acid sensitive (33). This organization and this behavior are similar to those of the Aps system of *Staphylococcus epidermidis*, which regulates the expression of the *dlt* operon, the *mprF* gene, and the *vraFG* ABC transporter in response to AMPs (34). We therefore renamed module 12 ApsRSAB, standing for antimicrobial peptide sensor.

In this report, we investigated the function of the ApsR-dependent orphan ABC transporter from *L. casei* BL23 in response to AMPs. A mutational study demonstrated

that the orphan transporter is a defensin-specific resistance transporter, which we therefore renamed DerAB, with DerA (locus *LCABL_21680*) forming the NBD (ATPase) and DerB (locus *LCABL_21670*) the MSD (permease) subunits of the system. Absence of a functional DerAB transporter not only increased the sensitivity to defensins but, remarkably, also resulted in a decreased sensitivity to nisin. This surprising finding could be explained by gene expression studies in a Δ*derB* mutant showing hyperactivation of the Psd- and Aps-regulated systems in response to nisin. Moreover, bacterial two-hybrid assays showed that DerB can interact with PsdS and PsdA. Based on these results, we propose that nonproductive protein-protein interactions of DerAB with the PsdRSAB sensory complex might result in regulatory interference within Psd module signal transduction that modulates the induction of the nisin resistance response.

RESULTS

DerAB mediates resistance against insect-derived defensins but renders *L. casei* nisin sensitive. ApsRSAB from *L. casei* BL23 is involved in resistance against several bacteriocins and the fungal peptide plectasin, and it controls the expression of the BceAB-like orphan transporter DerAB (32), which has so far not been studied with respect to its physiological role. Since all known BceAB-like transporters mediate AMP resistance (17), we tested the sensitivity of a Δ*derB* strain against a wide range of different AMPs. No differences in MIC values were obtained for bacitracin, mersacidin, and vancomycin when comparing the Δ*derB* strain with the parental strain BL23 (Table 1). While the absolute MIC values for plectasin ($>40\ \mu g \cdot ml^{-1}$) and subtilin (3% [vol/vol]) were also identical, the *derB* mutant showed slightly reduced growth in the presence of these peptides compared to that of the wild type (Fig. 2A and B, respectively). Surprisingly, the Δ*derB* strain was 10-fold more resistant to nisin than the parental strain (Fig. 2C). Since nisin and subtilin are structurally similar type A lantibiotics, these results were puzzling. We had previously shown that PsdAB from BL23 is involved in nisin and subtilin resistance (32); therefore, we reasoned that a contribution to resistance/sensitivity mediated by DerAB should be revealed in a double mutant Δ*derB* Δ*psdB* strain. For subtilin, we did not observe any significant contribution of DerAB to mediating resistance (the MIC of subtilin was 0.5% [vol/vol] for both the Δ*psdB* and Δ*derB* Δ*psdB* mutants). In contrast, the MIC of nisin was $0.5\ \mu g \cdot ml^{-1}$ for BL23, $0.3\ \mu g \cdot ml^{-1}$ for the more sensitive Δ*psdB* strain, and $5\ \mu g \cdot ml^{-1}$ for the highly resistant Δ*derB* strain, while the Δ*derB* Δ *psdB* mutant had an intermediate phenotype with an MIC of $1\ \mu g \cdot ml^{-1}$, making this double mutant more resistant to nisin than the wild type. These results demonstrate that a *derB* deletion could rescue the nisin sensitivity of a *psdB* mutant and corroborated the relevance of DerAB in the induction of a full nisin resistance response. A more detailed investigation of the nisin resistance phenotype of the Δ*derB* strain is described below.

Since *L. casei* strains can be found in the human gastrointestinal tract (35), where they are exposed to AMPs of the innate immune defense (36), we next tested the sensitivity of the strains to human AMPs. LL37 is a human cathelicidin (37) that functions as a specific activator of the Bce-like ApeRSAB (formerly YxdJKLM) module of *B. subtilis* (38, 39), while hBD1 is a human defensin that is activated by reduction of its disulfide bridges (40, 41). We did not observe any differences in sensitivity to LL-37 or hBD1 between the BL23 and Δ*derB* strains (Table 1). In contrast, strains carrying Δ*apsR*, Δ*apsB*, and Δ*dltA* mutations were more sensitive to LL-37 than was the BL23 wild type (see Fig. S1 in the supplemental material), indicating a role of ApsRSAB in resistance against LL-37, likely by regulating the activity of the Dlt system.

Lactobacilli can also be found in the microbiota of insects (42, 43). Next, we tested the sensitivity of the BL23 and Δ*derB* strains against a collection of 18 insect-derived AMPs. Both strains were resistant against even the highest concentrations of most insect AMPs tested (Table 1). However, for three defensins we could observe significant differences in resistance. The Δ*derB* mutant was slightly more sensitive to LSer-Def4 (BR090; Fig. 2D) and much more sensitive to sapecin A (BR080; MIC, $>160\ \mu g \cdot ml^{-1}$ for BL23 and $80\ \mu g \cdot ml^{-1}$ for the Δ*derB* strain) and Lser-Def3 (BR092; MIC, $>320\ \mu g \cdot ml^{-1}$

TABLE 1 Antimicrobial peptides used in this study and MIC values against *L. casei* BL23 and the Δ*derB* mutant

AMP	Class	APD3 ID no.[a]	Sequence	3D structure[b]	MIC[c] (15 h)	
					BL23	Δ*derB* mutant
Bacteriocins						
Bacitracin	Cyclic peptide	n.r.	ICLEIKOrnIFHDN[d]	Cyclic	10	10
Nisin A	Type A lantibiotic	AP00205	ITSISLCTPGCKTGALMGCNMKTATCHCSIHVSK	Non-$\alpha\beta$	0.5	5
Mersacidin	Type B lantibiotic	AP01206	CTFTLPGGGGVCTLTSECIC	Non-$\alpha\beta$	10	10
Subtilin	Type A lantibiotic	AP00206	WKSESLCTPGCVTGALQTCFLQTLTCNCKISK	Unknown	3	3 (¶)
Vancomycin	Glycopeptide	n.r.	n.f.[f]	Branched tricyclic	1.7	1.7
Fungal AMP						
Plectasin	Defensin	AP00549	GFGCNGPWDEDDMQCHNHCKSIKGYKGGYCAKGGFVCKCY	Combine-$\alpha\beta$	>40	>40 (¶)
Insect AMPs						
BR001 (cecropin A)	Cecropin	AP00139	KWKLFKKIEKVGQNIRDGIIKAGPAVAVVGQATQIAK*-NH2[e]	α	>320	>320
BR002 (sarcotoxin IA)	Cecropin A2	AP00230	GWLKKIGKKIERVGQHTRDATIQGLGIAQQAANVAATAR*-NH2	α	>320	>320
BR003 (cecropin A [insect: *Aedes aegypti*])	Cecropin	n.r.	GGLKKLGKKLEGAGKRVFNAAEKALPVVAGAKALRK	(α)	>320	>320
BR005 (stomoxyn)	Stomoxyn	AP00484	RGFRKHFNKLVKKVKHTISETAHVAKDTAVIAGSGAAVVAAT	α	>320	>320
BR044 (LSerStomox2)	Stomoxyn	AP02513	GFRKRFNKLVKKVKHTIKETANVSKDVAIVAGSGVAVGAAMG	(α)	>320	>320
BR080 (sapecin A)	Defensin	AP00227	ATCDLLSGTGINHSACAAHCLLRGNRGGYCNGKAVCVCRN	Combine-$\alpha\beta$	>160	80
BR081 (insect: *Aeschna cyanea*)	Defensin	AP00182	GFGCPLDQMQCHRHCQTITGRSGGYCSGPLKLTCTCYR	Bridge	>320	>320
BR087 (insect: *Lucilia sericata*)	Defensin	n.r.	ATCDLLSATGFSGTACAAHCLLIGHRGGYCNTKSVCVCRD	(Combine-$\alpha\beta$)	>400	>400
BR088 (lucifensin)	Defensin	AP01532	ATCDLLSGTGVKHSACAAHCLLRGNRGGYCNGRAICVCRN	Combine-$\alpha\beta$	>400	>400
BR089 (LSer-Def7)	Defensin	AP02507	FTCNSYACKAHCILQGHKSGSCARINLCKCQR	Bridge	>320	>320
BR090 (LSer-Def4)	Defensin	AP02505	LTCNIDRSFCLAHCLLRGYKRGFCTVKKICVCRH	Bridge	>400	>400 (¶)
BR091 (LSer-Def6)	Defensin	AP02506	GTCSFSSALCVVHCRVRGYPDGYCSRKGICTCRR	Bridge	>400	>400
BR092 (LSer-Def3)	Defensin	AP02504	ATCDLLSGTGANHSACAAHCLLRGNRGGYCNSKAVCVCRN	Bridge	>320	320
BR097 (cecropin A [*Galleria mellonella*])	Cecropin	AP03067	KWKIFKKIEKAGRNIRDGIIKAGPAVSVVGEAATIYKTG*-NH2	(α)	>320	>320
BR098 (ecropin B [*G. mellonella*])	Cecropin	AP03068	KWKFFKKIERVGQNIRDGIIKAGPAVQVVGQAATIYKGK*-NH2	(α)	>320	>320
BR099 (cecropin C [*G. mellonella*])	Cecropin	AP03069	RWKVFKKIERMGQHIRDGIIKAGPAVAVVGQASTIISG*-NH2	(α)	>320	>320
BR100 (Gm cecropin D-like peptide)	Cecropin D	AP00755	ENFFKEIERAGQRIRDAIISAAPAVETLAQAQKIIKGGD*-NH2	(α)	>320	>320
BR101 (Et-Cec1 [*Eristalis tenax*])	Cecropin	n.r.	GFLKKIGKKLEGAVQRTRDATIQTIAVAQAAANVAATAKQG	(α)	>320	>320
Human AMPs						
LL37	Cathelicidin	AP00310	LLGDFFRKSKEKIGKEFKRIVQRIKDFLRNLVPRTES	α-helix	>27	>27
hBD-1	Defensin	AP00451	DHYNCVSSGGQCLYSACPIFTKIQGTCYRGKAKCCK	Combine-$\alpha\beta$	>20	>20

[a]Antimicrobial Peptide Database (APD3) (8) identification (ID) number. n.r., not registered in APD3.

[b]Three-dimensional (3D) structure as annotated in APD3 based in (73): α, AMPs with helical structures; combine-$\alpha\beta$, AMPs with α-helical and β-strands in the 3D structure; non-$\alpha\beta$, contains neither α-helical nor β-strands; bridge, AMPs without 3D structure determined, disulfide-linked, usually β-structure. When no structural data were available, structure prediction was made using the Swiss-Model webpage (https://swissmodel.expasy.org/) (67) and is indicated in parentheses.

[c]MIC are in $\mu g \cdot ml^{-1}$ except those for subtilin (% [vol/vol]) and vancomycin (mg/ml). ¶ indicates that the mutant was more sensitive when assayed for final cell densities (see Fig. 2).

[d]Sequence of linear peptide precursor; bond between Lys_6 and Asn_{12}. Orn, D-ornithine.

[e]*, C-terminal amidation (see Materials and Methods for further details).

[f]n.f., not found.

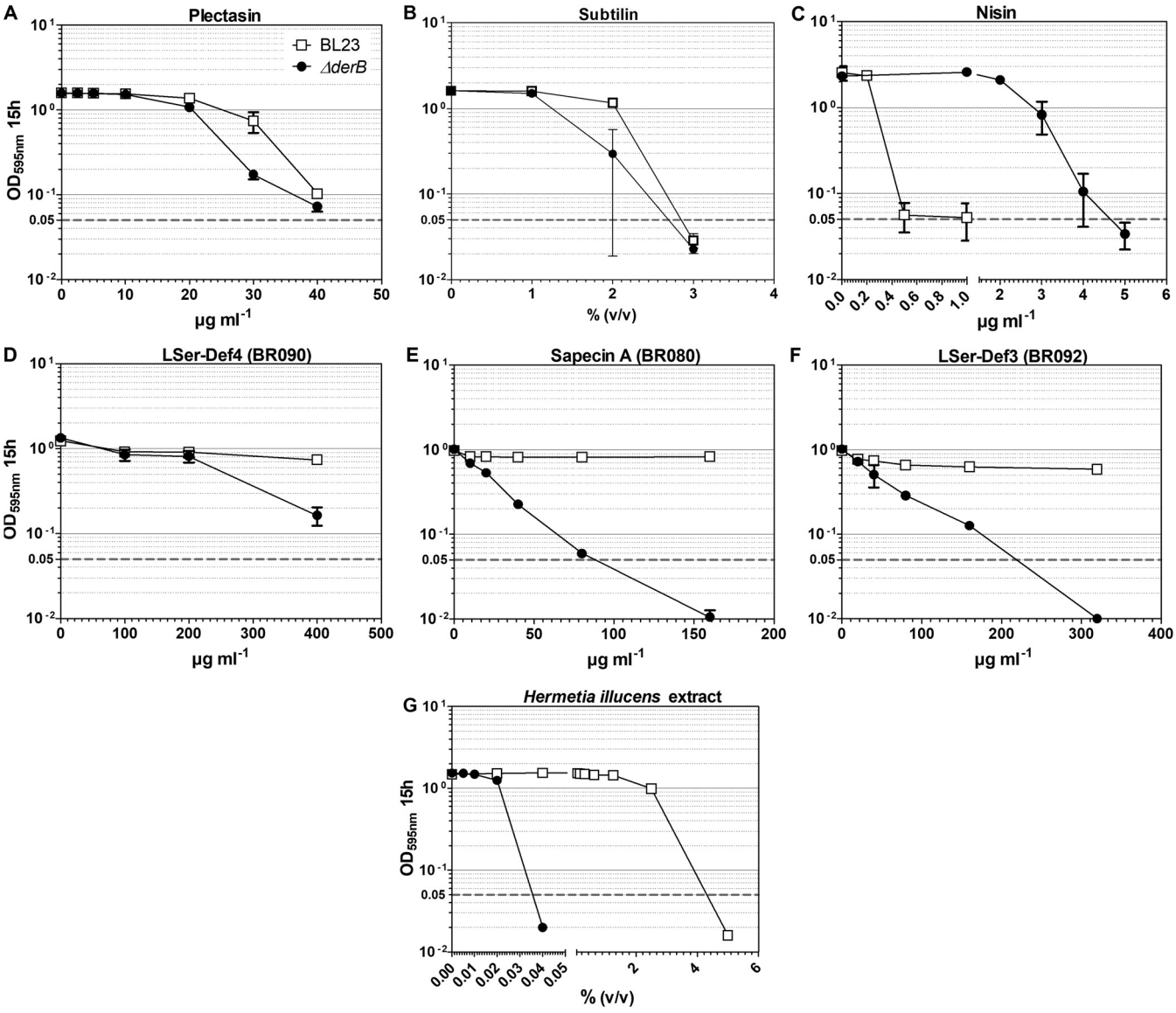

FIG 2 MICs of different AMPs for *L. casei* BL23 (white squares) and Δ*derB* strains (black circles). (A) Plectasin. (B) Subtilin. (C) Nisin. (D) LSer-Def4 (BR090). (E) Sapecin A (BR080). (F) LSer-Def3 (BR092). (G) Extract from *Hermetia illucens* larvae. Strains were inoculated to an optical density at 595 nm (OD_{595}) of 0.05 (dashed line) in MRS with different concentrations of antibiotics. Final OD_{595} readings were taken after 15 h of incubation at 37°C (OD_{595nm} 15h). MIC (see Table 1) was defined at the lowest antibiotic concentration where the final OD was at or below the starting OD. Means and standard deviations from at least duplicates are presented. A representative result from *H. illucens* extract is presented because due to the preparation procedure, the absolute potencies of the extracts (as expressed in %) differ significantly between individual preparations, but the relative sensitivities were very well reproduced in independent assays.

for BL23 and 320 μg · ml^{-1} for the Δ*derB* strain) (Fig. 2E and F, respectively) than was the parental strain, indicating that DerAB mediates resistance against these compounds. To confirm that the observed phenotype was specific to and directly caused by the loss of DerAB, we repeated the sensitivity experiment for sapecin A on a strain carrying an ectopic copy of *derB* to complement the Δ*derB* mutation. Indeed, complementation restored much of the original resistance (see Fig. S2 in the supplemental material). The slight remaining differences from the wild type are likely due to altered expression levels of *derB* between the native and ectopic copy, as was observed for complementation of a *bceB* mutant of *B. subtilis* (44). Taken together, the data indicate that DerAB specifically mediates resistance against insect-derived AMPs.

Subsequent microscopic studies revealed significantly different morphological aberrations in the Δ*derB* strain when challenged with different AMPs (Fig. 3; see also Table S1 in the supplemental material). No morphological differences were found between

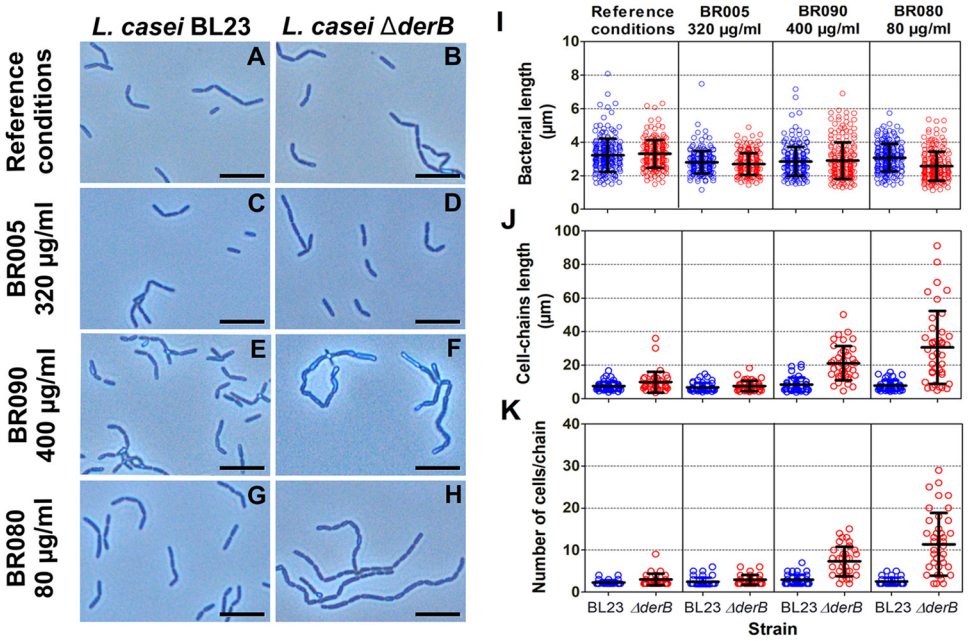

FIG 3 Sensitivity phenotypes of the Δ*derB* strain are associated with morphological changes. (A to H) Microscopic characterization after AMP exposition. Stationary-phase cell cultures of BL23 (left column pictures) and the Δ*derB* strain (right column pictures) grown for 24 h under reference conditions (A and B) or in the presence of insect-derived AMPs were photographed (phase contrast, ×40 magnification). Selected AMPs were chosen as representative of different sensitivities of the Δ*derB* strain relative to those of the wild type (see Table 1). The sensitivity phenotypes were similar for BR005 at 320 μg · ml^{-1} (C and D). The Δ*derB* strain was slightly more sensitive than BL23 for BR090 at 400 μg · ml^{-1} (E and F). The mutant was much more sensitive than the wild type for BR080 at 80 μg ml^{-1} (G and H). Bar, 10 μm. (I to K) Quantification of the morphological changes associated with the sensitivity phenotypes. (I) Average bacterial length (μm; $n = 200$), (J) average cell chain length (μm; $n = 40$ cell chains), and (K) average number of cells per chain ($n = 40$ cell chains) of the stationary-phase cell cultures photographed in panels A to H were determined. BL23 and the Δ*derB* strain are depicted with blue and red circles, respectively. Means and standard deviations are indicated with the horizontal and the barred vertical black lines, respectively. For a detailed statistical analysis of the results, see Table S1 in the supplemental material.

the BL23 and Δ*derB* strains after exposure to BR005 (Fig. 3C and D), BR081, BR087, BR088, BR091, or subtilin 2% (vol/vol) (data not shown). In contrast, the Δ*derB* strain was strongly affected after exposure to 400 μg · ml^{-1} BR090, showing chaining (Fig. 3J and K), aberrant morphologies, and cells becoming phase transparent (Fig. 3F). Although minor changes were also observed in the wild type treated with BR090, these were far less pronounced (Fig. 3E). After incubation with BR080 (Fig. 3G and H) or BR092 (data not shown), the chaining phenotype of the *derB* deletion mutant was even more pronounced (Fig. 3J and K), while the parental strain remained unaffected. These morphological changes of the Δ*derB* strain after exposition to BR080, BR090, and BR092 are in good agreement with the sensitivity phenotypes observed for these AMPs (Fig. 2).

L. casei apsRSAB mutants are defective in D-alanylation of teichoic acids, resulting in a more negative surface charge and a higher AMP sensitivity of the Δ*apsR*, Δ*apsB*, and Δ*dlt* strains than those of the parental strain (32). A possible explanation for the observed sensitivity of the Δ*derB* strain could therefore be that DerAB somehow contributes to the regulation of the Dlt system through ApsRS. However, measurements of the cell surface charge by cytochrome *c* binding assays (32, 45) did not show any significant differences between BL23 and the Δ*derB* strain (see Fig. S3 in the supplemental material), thereby ruling out this cause for the higher AMP sensitivity of the *derB* mutant.

Since the Δ*derB* strain showed the strongest sensitivity phenotypes when exposed to insect-derived defensins (Fig. 2E and F), we additionally investigated the contribution of DerAB to resistance against crude extracts derived from larvae of the dipteran species black soldier fly *Hermetia illucens* (see Materials and Methods for their prepa-

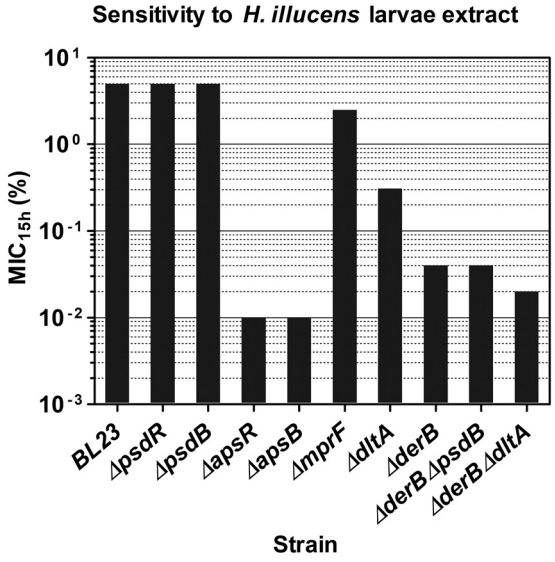

FIG 4 Sensitivities to *H. illucens* larval extracts. Different layers of resistance against AMPs from *H. illucens*. MIC at 15 h (expressed as % [vol/vol] of initial extract) of *H. illucens* larval extract against *L. casei* BL23 and derivative strains. A representative data set is shown. Due to the preparation procedure, the absolute potencies of the extracts (expressed in %) differ significantly between individual preparations, but the overall relative sensitivities were very well reproduced in independent assays.

ration), which are particularly prolific sources of broad-spectrum antimicrobial substances (46). A recent transcriptome study identified 53 genes encoding putative AMPs from different families, half of which are putative defensins (47). Among those, the defensin-like peptide 2 (DLP2; ATCDLLSPFKVGHAACALHCIAMGRRGGWCDGRAVCNCRR) and the defensin-like peptide 4 (DLP4; ATCDLLSPFKVGHAACAAHCIARGKRGGWCDKRA VCNCRK) have been characterized (48, 49). Both defensins possess a CS$\alpha\beta$ structure and are active against Gram-positive bacteria. If DerAB is a defensin-specific resistance transporter, its absence should render *L. casei* also sensitive to *H. illucens* extracts. Indeed, the Δ*derB* strain was over 100-fold more sensitive than the parental strain (Fig. 2G; MIC is 5% [vol/vol] for BL23 and 0.04% [vol/vol] for the Δ*derB* strain), thereby confirming its role in conferring resistance against AMPs produced by *H. illucens*. Besides the strong effect on resistance, we observed some morphological differences in the forms of elongated and chaining cells in the Δ*derB* strain after exposition to *Hermetia* larvae extracts (see Fig. S4 in the supplemental material).

ApsRSAB regulates different layers of resistance against antibiotics produced by *H. illucens* larvae. The AMP resistance determinants of *L. casei* are controlled by the Psd and Aps modules; the PsdRSAB system regulates the target operon *psdAB*, and the ApsRSAB system regulates the expression of the *dlt* operon, *mprF* gene, and *derAB* transporter (32) (Fig. 1). Because of the potency of the *H. illucens* larval extracts and the strong difference in sensitivity between the *derB* deletion mutant and the parental strain, we next aimed at analyzing the hierarchy within the AMP resistance network orchestrated by the Psd and Aps modules and the individual contributions of their target genes to protecting *L. casei* against the combined challenge of *H. illucens* extracts. Towards this goal, we performed a comprehensive mutational study of the individual components of the AMP resistance network of *L. casei* (Fig. 4).

The MIC values for the Δ*psdR* and Δ*psdB* strains were similar to that of the wild-type strain BL23 (5% [vol/vol]), indicating that the stand-alone Psd module is not involved in mediating resistance against larval extracts (Fig. 4). In contrast, both mutants that rendered the Aps system dysfunctional, the Δ*apsR* and Δ*apsB* strains, were highly sensitive to *H. illucens* extracts, with an MIC of 0.01% (vol/vol) (500-fold more sensitive than the wild type).

Next, we determined the MIC for all three Aps-dependent AMP resistance determinants deleted individually. While both the Δ*mprF* and Δ*dltA* mutants showed a slight

increase in sensitivity compared to that of the wild type, the most marked effect was again observed in the Δ*derB* strain (Fig. 4). These data clearly show that the DerAB transporter provides the primary resistance layer against the AMPs present in the larval extract, while D-alanylation of teichoic acids and—to a smaller extent—the L-lysinylation of phospholipids represent a secondary layer of resistance. In agreement with this hierarchy, the MIC of a Δ*derB* Δ*dltA* double mutant (0.02% [vol/vol]) was further increased compared to those of the single mutants, that is, the double mutant was 16-fold more sensitive than the Δ*dltA* strain and 2-fold more sensitive than the Δ*derB* strain. To rule out any minor contributions to resistance by the Psd system, we also tested a Δ*derB* Δ*psdB* double mutant, but we could not detect any changes relative to the Δ*derB* single mutant. Taken together, our results demonstrate that a clear hierarchical organization of multiple layers ensures the protection of *L. casei* against insect-derived AMPs, and all resistance determinants relevant for counteracting the AMPs contained in *H. illucens* extract are under the control of a single module, ApsRSAB.

Resistance determinant genes are transcriptionally overexpressed in the Δ*derB* strain in response to nisin. As mentioned above, the Δ*derB* strain unexpectedly showed a 10-fold increase in resistance against nisin (MIC, 5 μg · ml^{-1}; MIC for parental strain, 0.5 μg · ml^{-1}) (Table 1 and Fig. 2C). PsdAB is involved in nisin resistance and partially contributes to the hyperresistance of the Δ*derB* strain (MIC value for the Δ*derB* Δ*psdB* double mutant, 1 μg · ml^{-1}). However, the main nisin resistance determinant of *L. casei* is the Dlt system, since the Δ*dltA* mutant was 12.5-fold more sensitive to nisin than the wild type (MIC for Δ*dltA* strain, 0.04 μg · ml^{-1}) (32). We have previously shown that transcription of the *psdAB* and *dltA* genes is induced in a nisin-dependent manner in BL23, as are the genes *derAB* and *mprF* (32). We therefore hypothesized that the increased resistance of the Δ*derB* strain might be due to a higher expression level of the nisin resistance determinants in this mutant. Thus, we tested the response of these genes following nisin exposure in the Δ*derB* strain background compared to that in the wild type, following the previously established procedure (32).

Expression of *psdR*, *apsB*, *apsA*, and *apsR* was not induced by nisin in either strain (Fig. 5A), in agreement with the role of PsdRS and ApsRSAB in signaling rather than resistance (32). Strikingly, nisin exposure of the Δ*derB* strain led to a notable increase of induction of nisin resistance genes compared to that in the BL23 wild type (Fig. 5A); the genes encoding the transporters (*psdA*, *psdB*, and *derA*) were up to 10-fold more strongly induced in the Δ*derB* strain than in the wild type. Likewise, *dltA* and *mprF* also responded more strongly (~2.5-fold and ~3.5-fold, respectively) in the mutant. Importantly, no significant differences in gene expression were found between the Δ*derB* strain and the parental strain under reference conditions (see Fig. S5 in the supplemental material), showing that the increased induction was due to a hyperresponse to nisin exposure and not to general changes in gene expression upon *derB* deletion. Moreover, since the systems involved in nisin resistance in *L. casei* BL23 also mediate subtilin resistance (32), we next tested the response of these genes following subtilin exposure in the Δ*derB* strain background compared to that of the wild type. Noticeably, no significant differences in gene expression were found between the Δ*derB* strain and the parental strain in response to subtilin (Fig. 5B; see also Fig. S5 in the supplemental material). We therefore concluded that the increased nisin resistance of the Δ*derB* strain was due to an overexpression, compared to the parental strain, of the nisin resistance determinants *psdAB*, *mprF*, and the *dlt* operon, and that this response was specific for nisin.

DerAB may interfere with signaling through spurious protein-protein interactions. We next investigated the molecular basis for the observed hyper-induction of nisin resistance genes in the Δ*derB* strain. For the BceRSAB system of *B. subtilis*, it is known that signaling depends on a sensory complex formed between the transport permease BceB and the histidine kinase BceS (20). Moreover, signaling requires a functional transporter that is capable of ATP hydrolysis (25, 44), i.e., correct interaction between the permease BceB and the ATPase (BceA) subunits. Since it could be possible that DerAB may somehow interfere with one or more of the nisin-responsive signaling

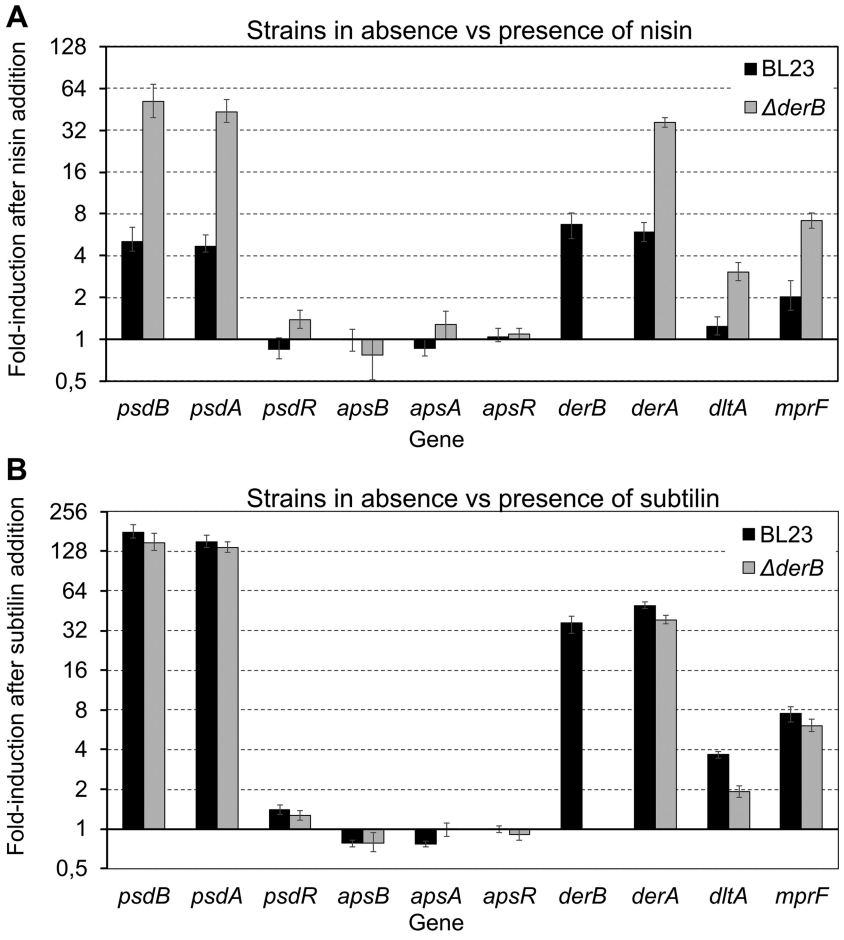

FIG 5 Expression of known AMP resistance determinants in *L. casei* BL23 and the Δ*derB* mutant after nisin (A) and subtilin (B) addition. Transcript levels were determined by real-time RT-PCR 10 min after addition of 22.5 ng · ml^{-1} nisin (A) and 1% (vol/vol) subtilin (B). Induction (*x*-fold) was calculated relative to transcript levels in the same strain under reference conditions. Data are shown as means ± standard errors from at least six replicates.

pathways in the cell, we performed bacterial two-hybrid experiments of all involved protein partners to test if the permease DerB is able to interact with any of the components of the Psd or Aps resistance systems (Fig. 6; see also Fig. S6 in the supplemental material). In addition to the expected interaction between DerB and DerA, we also obtained positive results for DerB paired with PsdA (Fig. 6). It is possible that such noncognate binding of the ATPase PsdA by DerB may reduce the ability of the PsdAB transporter to trigger signaling via PsdS. Moreover, we observed clear interactions between DerB and PsdS (Fig. 6). It is likely that such noncognate interactions between the permease DerB and the Psd histidine kinase would interfere with

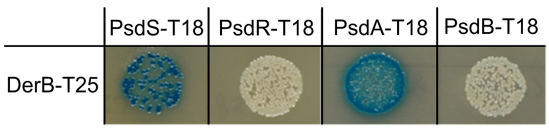

FIG 6 Bacterial two-hybrid analysis of the interactions of DerB with the PsdRSAB module. C-terminal and N-terminal translational fusions of the T18 and T25 domains of the adenylate cyclase CyaA of *Bordetella pertussis* were created for each protein individually. Different hybrid fusions were tested in pairwise combinations in *E. coli* BTH101. The cells were spotted onto LB plates containing X-Gal (100 μg · ml^{-1}), IPTG (1 mM), and antibiotics for selection. Pictures were taken after 48 h of incubation at 30°C. The blue colonies indicate positive interaction results. For clarity, only a single representative pair is shown in the figure. See Fig. S6 in the supplemental material for the complete set of combinations.

native signaling. Relief of this interference in the Δ*derB* strain could then explain the observed increase in the amplitude of the nisin response and resulting nisin resistance.

Unfortunately, similar bacterial two-hybrid experiments with the Aps proteins were less conclusive because several of the fusion constructs did not even give positive results with their known interaction partners (Fig. S6); consequently, these assays were not informative for potential interactions between DerAB and the Aps system.

DISCUSSION

ABC transporters acting as detoxification mechanisms are of major importance as AMP resistance systems in *Firmicutes* species (17). In this study, we unraveled the function of DerAB in *L. casei* BL23, which belongs to the BceAB-like group of transporters.

Our results demonstrate that from the available panel of antimicrobial compounds, four CS$\alpha\beta$ defensins (plectasin, sapecin A, LSer-Def4, and LSer-Def3) are the most relevant substrates of DerAB. Such defensins are ubiquitously produced in plants, insects, mussels, and fungi, and they form an important component of innate immunity (10). In addition to demonstrating that DerAB confers resistance to defined compounds, we demonstrated the relevance of DerAB for the survival of *L. casei* when challenged with a potent mix of insect AMPs from *H. illucens* larvae. Lactobacilli grow in a variety of nutrient-rich carbohydrate-containing habitats. In addition to having well-known roles in fermentation and the spoilage of food, *L. casei* is found in the oral cavity and in the gastrointestinal and genital tracts of humans and other animals (50). Moreover, different *Lactobacillus* species have been found in the microbiota of insects (42, 43). It is usually assumed that lactobacilli present in food come from the food processing equipment, raw foodstuffs such as plant material, or fecal contamination, but it appears that insects may play a role in the dissemination of *L. casei*. A recent study has provided evidence suggesting that insects are the natural reservoir of *Lactobacillus sanfranciscensis*, an organism involved in sourdough fermentation (51). Interestingly, in this study, operational taxonomic units (OTUs) belonging to the *L. casei* group were the second most numerous after *L. sanfranciscensis* within lactobacilli OTUs (51). Our results suggest that possession of DerAB may protect *L. casei* in different AMP-enriched environments of eukaryotic origin, including insects, and thereby enable it to colonize its hosts.

Furthermore, by testing the sensitivity of our collection of mutants to extracts from *H. illucens* larvae, which contain a very potent mixture of AMPs (46, 47), we showed that BL23 possesses several layers of AMP resistance. In this network, DerAB is the defensin-specific primary resistance mechanism, while the Dlt system and MprF protein constitute the secondary, more general resistance layer by altering the bacterial surface charge (Fig. 1). Remarkably, in *Bacillus subtilis*, the response to bacitracin also consists of a hierarchy of different layers of resistance; specifically, the BceAB transporter constitutes the primary (drug-sensing and highly efficient) resistance determinant, and the LiaIH system and the BcrC phosphatase constitute the secondary (damage-sensing and less efficient) layer of resistance (52). Thus, a clear hierarchical organization of multiple layers ensure protection of both *L. casei* and *B. subtilis* against AMPs. Interestingly, not only are the individual components of the resistance networks different between *L. casei* (DerAB transporter, Dlt operon, and MprF protein) and *B. subtilis* (BceAB transporter, LiaIH system, and BcrC phosphatase) (52); the resistance layers are also controlled by separate cell envelope stress systems in *B. subtilis* (52), whereas all resistance determinants relevant for counteracting the AMPs contained in *H. illucens* extract are under the control of a single module, ApsRSAB, in *L. casei*.

So far, the substrate specificity of BceAB-like transporters has not been related with any particular feature of the respective AMPs (17, 21, 28). Our results for DerAB indicated a preference for CS$\alpha\beta$ defensins, e.g., plectasin, sapecin A (BR080), LSer-Def4 (BR090), and LSer-Def3 (BR092). Surprisingly, DerAB does not confer resistance against the structurally closely related defensins lucifensin (BR088), BR081, BR087, LSer-Def7 (BR089), and LSer-Def6 (BR091) (Table 1). This indicates that DerAB can distinguish

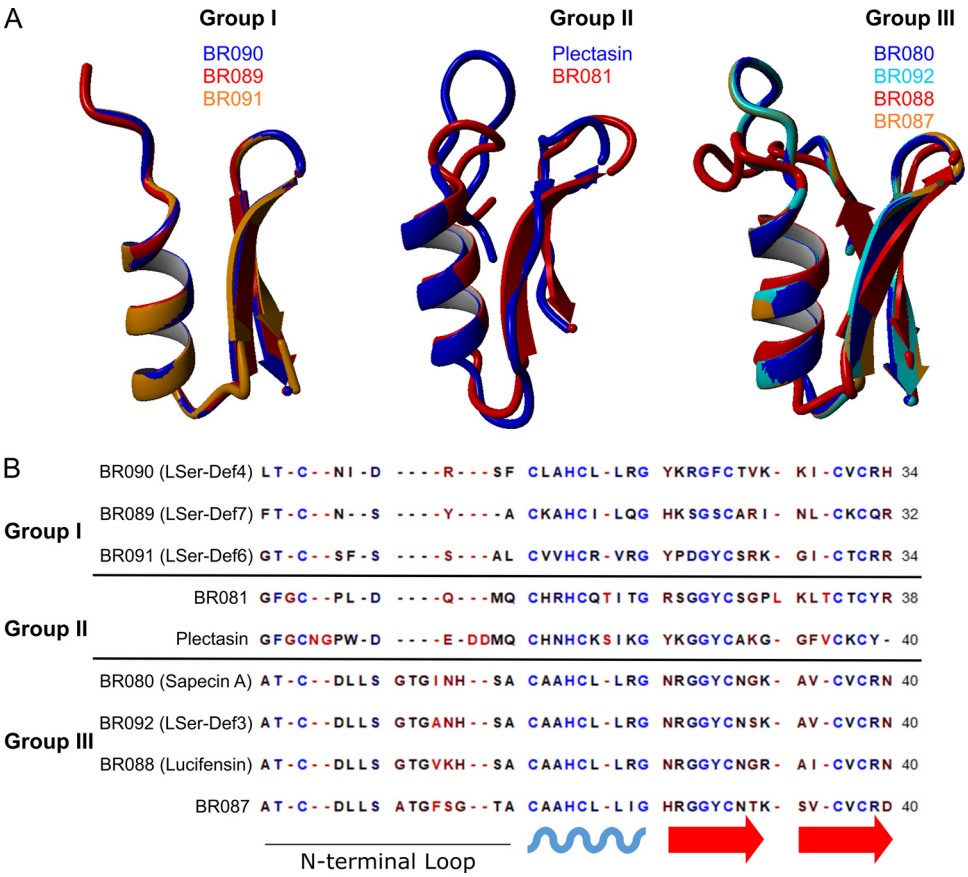

FIG 7 Structure and sequence comparison of defensins grouped according to loop size and loop sequence similarity. (A) Structural alignment of defensins. Substrates of the DerAB transporter are colored blue and cyan; nonsubstrates are colored red and orange. (B) Sequence alignment. Residues are colored according to conservation from 0% (red) to 100% (blue). The N-terminal loop and the secondary structure elements (blue wave, α-helix; red arrow, β-sheet) are indicated under the alignment.

between very similar CS$\alpha\beta$ defensin substrates, a situation reminiscent of the results obtained for the Psd module of *B. subtilis* (29). We performed a structural analysis of all tested candidates mentioned above to further investigate this apparent specificity of DerAB for some defensins (Fig. 7). The investigated defensins show moderate sequence conservation with an average sequence identity of 50% (see Fig. S7 in the supplemental material). The overall structure of the defensins is well conserved, with all available structures harboring a cysteine-stabilized α-helix–β-sheet (CS$\alpha\beta$) motif. The main structural deviations are in the N-terminal loop region, which is also least well conserved, with respect to both its size and its amino acid sequence (Fig. 7). No obvious pattern of structural determinants distinguishing substrates from nonsubstrates could be extracted, in line with previous studies on the substrate specificity of BceAB-like transporters (21).

The most puzzling result that we obtained during our initial sensitivity screen was the hyperresistance of the *derB* deletion mutant against the lantibiotic nisin. Transcriptional studies in the Δ*derB* strain in response to nisin demonstrated that the absence of this transporter resulted in an overinduction of *mprF*, the *dlt* operon, and *psdAB*. Both the Dlt system and the PsdAB transporter are crucial for nisin resistance in *L. casei* (32). Our results strongly suggest that their overexpression accounts for the hyperresistance of the Δ*derB* strain to nisin. This hypothesis is supported by independent studies in other *Firmicutes* bacteria that demonstrated the role of *dlt* expression levels for AMP resistance. Acquisition of nisin resistance in *Lactococcus lactis* IL1403 was partly due to higher expression levels of the *dlt* operon (53). Similarly, strains of *Staphylococcus*

aureus Sa113 bearing additional copies of the *dlt* operon showed an increased level of D-alanine in LTA and WTA, which led to an increased nisin resistance (45).

In the case of the Δ*derB* strain investigated here, increased nisin resistance could, however, not be explained by acquisition of additional copies of resistance genes. Instead, we could show that DerB has the ability to interact with components of the Psd resistance system. We propose that such spurious interactions with noncognate protein partners likely have a negative impact on signal transduction. That is, in the presence of nisin, not all PsdS histidine kinases receive a signal from their cognate transporter PsdAB, because a proportion are in a nonproductive complex with DerB. This interference is removed upon *derB* deletion, allowing the full potential activation of *psdAB* expression and thus a greater level of resistance against the AMP. Of note, whereas the strain C-*derB*, carrying an ectopic copy of *derB* in the *derB* deletion mutant background, complemented sensitivity to the defensin sapecin A, the restoration of nisin sensitivity was only very weak (see Fig. S2 in the supplemental material). It is likely that the ectopic copy of *derB* did not result in the same protein levels of DerB in the cell and therefore interference with normal Psd signaling was not observed. However, indirect evidence supporting this interference model is available. Results of gene expression previously reported (32) for mutants defective in the ApsRSAB system, and results reported here for the Δ*derB* strain (Fig. 5A and Fig. S5), showed an increase in expression of *psdAB* in the presence of nisin, suggesting that a decrease in the ratio of DerAB to PsdAB results in increased PsdRSAB signal transduction. Furthermore, results obtained with subtilin (Fig. 5B and Fig. S5) show that this is a nisin-specific effect. To our knowledge, such a negative effect of one Bce-like resistance system on the function of another has not been previously reported. Also, why this phenotype is observed with nisin and not with a closely related lantibiotic such as subtilin is still unclear.

We previously showed that Bce-like systems are widespread among *Firmicutes* bacteria and that many species contain multiple copies with different substrate specificities (21). Often, the closest homolog to a given system is found in a different species, whereas the paralogs within a single species can be quite distantly related (21). For the Bce-like systems characterized to date, signaling between transporter and two-component system appears to be highly specific, and no accidental cross talk has been reported. The example of DerAB reported here may constitute an interesting evolutionary intermediate where the interaction specificity is not yet completely insulated, allowing nonproductive interference with the Psd system. In this scenario, in the presence of nisin, the interference by DerAB should pose a significant fitness burden on the cell. However, we did not observe any effects of a *derB* deletion on gene expression when cells were grown in unchallenged reference conditions or after subtilin exposure (Fig. 5B and Fig. S5), suggesting that DerAB has no negative effect in most situations. An alternative scenario could then be that the interference by DerAB is in fact beneficial to prevent an overreaction to nisin that could also pose a fitness burden to the cell. Interestingly, a similar hidden potential in the response to nisin mediated by Bce-like systems was also previously reported in *S. aureus* (54). While beyond the scope of the present study, it would be interesting to investigate if, under suitable experimental pressure, *L. casei* BL23 could evolve increased signaling specificity and circumvent the interference from DerAB.

In summary, in this work we demonstrated that DerAB is a defensin-specific resistance transporter that constitutes a primary layer of the *L. casei* cell envelope stress response. Its expression is controlled by the Aps module that also regulates the secondary, more general, layers of resistance, the Dlt system and MprF. Given the high degree of protection against insect-derived AMPs, it appears likely that the physiological role of DerAB is in host-microbe interactions and may allow *L. casei* to avoid innate immune defenses to colonize its eukaryotic hosts.

MATERIALS AND METHODS

Bacterial strains, plasmids, and grown conditions. Tables 2 and 3 list the strains and plasmids, respectively, used in this study. *Escherichia coli* DH10β and *Lactococcus lactis* MG1363 were used as

TABLE 2 Bacterial strains used in this study

Strain	Description[a]	Source or reference
E. coli DH10β	F$^-$ *mcrA* Δ(*mrr-hsdRMS-mcrBC*) Φ80*dlacZ*Δ*M15* Δ*lacX74 endA1 recA1 deoR* Δ(*ara-leu*)7697 *araD139 galU galK nupG rpsL* λ^-	Stratagene
E. coli BTH101	F$^-$, *cya-99, araD139, galE15, galK16, rpsL1* (Str^r), *hsdR2*, *mcrA1*, *mcrB1*	Lab collection
L. lactis MG1363	Plasmid-free derivative of NCDO712	74
L. casei BL23	Wild type	B. Chassy, University of Illinois
L. casei Δ*psdR*	BL23 Δ*LCABL_16430*	32
L. casei Δ*apsR*	BL23 Δ*rrp1* (*LCABL_19600*)	31
L. casei Δ*derB*	BL23 Δ*LCABL_21670*	This study
L. casei C-Δ*derB*	BL23 Δ*LCABL_21670* harboring plasmid *pT1*-RBS$_{derB}$*derB* Ery^r	This study
L. casei Δ*psdB*	*LCABL_16400* mutant; *pRV16400* Ery^r	32
L. casei Δ*apsB*	*LCABL_19580* mutant; *pRV19580* Ery^r	32
L. casei Δ*dltA*	*LCABL_08550* (*dltA*) mutant; *pRV08550* Ery^r	32
L. casei Δ*mprF*	*LCABL_24490* mutant; *pRV24490* Ery^r	32
L. casei Δ*derB* Δ*psdB*	BL23 Δ*LCABL_21670*; *LCABL_16400* mutant, *pRV16400* Ery^r	This study
L. casei Δ*derB* Δ*dltA*	BL23 Δ*LCABL_21670; LCABL_08550* (*dltA*) mutant, *pRV08550* Ery^r	This study

[a]Ery^r, erythromycin resistance; Str^r, streptomycin resistance.

intermediate hosts for cloning purposes. *E. coli* strains were grown in LB medium at 37°C with aeration. *L. lactis* strains were grown in M17 medium supplemented with 0.5% (wt/vol) glucose at 30°C under static conditions. *L. casei* strains were grown in MRS broth (Oxoid) at 37°C under static conditions. Agar (1.5% [wt/vol]) was added to prepare the corresponding solid medium. Strains were stored at −80°C in their corresponding growth media containing 20% (vol/vol) glycerol. Ampicillin at 100 μg · ml^{-1} was added to *E. coli* cultures, and erythromycin at 5 μg · ml^{-1} was added to *L. lactis* and *L. casei* cultures when required.

Construction of mutants. Oligonucleotides used in this study are listed in Table 4. Cloning in *E. coli* was performed following standard methods (55). *E. coli* strains were transformed by electroporation with a Gene Pulser apparatus (Bio-Rad), as recommended by the manufacturer; *L. lactis* strains were transformed by electroporation (56) and *L. casei* strains were transformed as described previously (57).

For a complete deletion of gene *LCABL_21670* (Δ*derB*) from *L. casei* BL23, two DNA fragments of approximately 700 bp upstream and downstream of the target gene were amplified from genomic DNA using primer pairs RG062-063 and RG064-065 (see Table 4). All subsequent steps of mutant construction were performed as previously described (32). Strain C-*derB* with the complementation of the *derB* deletion was achieved by cloning the corresponding gene and potential ribosome binding site (12-bp intergenic region between *derA* and *derB*), with primer pair RG220-221 (SpeI and BglII restriction sites; Table 4), under the constitutive P1 promoter in the expression vector *pT1NX* (58). The resulting plasmid, *pT1-RBS$_{derB}$derB* (Table 3), was used to transform *L. lactis* MG1363, and transformants were checked by sequencing of the inserted fragment. Subsequently, plasmid *pT1-RBS$_{derB}$derB* was used to transform *L. casei* Δ*derB*, resulting in strain *L. casei* C-Δ*derB* (Table 2), which was maintained with erythromycin selection.

Δ*derB* Δ*dltA* and Δ*derB* Δ*psdB* double mutant strains were obtained by insertional inactivation of the genes *LCABL_08550* (*dltA*) and *LCABL_16400* (*psdB*), respectively, in an *L. casei* Δ*derB* mutant background. A procedure similar to that previously described to obtain insertionally inactivated single mutants of genes *LCABL_08550* and *LCABL_16400* was followed (32).

Bacterial two-hybrid assays. We constructed C-terminal and N-terminal translational fusions of the T18 and T25 domains of the adenylate cyclase CyaA of *Bordetella pertussis* for each protein individually (40 constructs; Table 3), to test protein-protein interactions between DerAB and the PsdRSAB module, and between DerAB and the ApsRSAB module. Fusions were tested in pairwise combinations in *E. coli* BTH101 (59). For each cotransformation mixture, 3 × 10 μl aliquots were spotted onto LB agar plates containing 1 mM isopropyl-β-D-1-thio-galactopyranoside (IPTG) and 100 μg · ml^{-1} 5-bromo-4-chloro-3-indolyl-β-D-galactopyranoside (X-Gal) with selection for ampicillin and kanamycin resistance. Plates were incubated at 30°C for 48 h. Positive interaction results were identified by the formation of blue colonies.

Source or preparation of eukaryotic AMPs and subtilin. HBD-1 and LL-37 were purchased from Sigma-Aldrich (SRP3011 and 94261, respectively) and were reconstituted according to the manufacturer's instructions. The insect AMPs shown in Table 1 were selected according to their reported structural and functional properties, synthesized and purified to >95%. Cecropin 1 (from *Eristalis*) was synthesized by Pepmic Suzhou (Jiangsu, China). Cecropin A (from *Hyalophora* and *Aedes*), stomoxyn (from *Stomoxys*) and sarcotoxin IA were synthesized by JPT Peptide Technologies GmbH (Berlin, Germany). The rest of the peptides were synthesized by Covalab S.A.S. (Villeurbanne, France), based on the sequence of the mature peptides. All peptides were lyophilized for storage and were resuspended and diluted in double-distilled water. Excluding *Aedes* and *Eristalis* cecropins, all other cecropins and *Stomoxys* stomoxyn were modified by C-terminal amidation.

Larvae of the black soldier fly (*Hermetia illucens*) were obtained from a pilot rearing plant in Grimma (Saxony, Germany) and grown at 24°C in the laboratory. *H. illucens* larvae were induced as previously described (39, 46) by injecting a fungal spore suspension (spores of *Verticillium lecanii* and *Metarhizium anisopliae*) into the hemolymph and by feeding a bacterial mix (*E. coli*, *Micrococcus luteus*, *Pseudomonas fluorescens*, and *B. subtilis*) to simulate an infection and boost AMP production. The larvae were pricked

TABLE 3 Vectors and plasmids used in this study

Vector or plasmid	Description[a]	Source or reference
pRV300	Insertional vector for *Lactobacillus*; Amp^r, Ery^r	75
pT1NX	Expression vector for Gram-positive bacteria harboring the constitutive P1 promoter; Ery^r	58
pRVOrPe-del	*pRV300* containing fused flanking fragments upstream and downstream of *LCABL_21670*	This study
pRV08550	*pRV300* containing a 679-bp internal fragment of *LCABL_08550* (*dltA*)	32
pRV16400	*pRV300* containing a 975-bp internal fragment of *LCABL_16400* (*psdB*)	32
pT1-RBS$_{derB}$derB	*pT1NX* with cloned *LCABL_21670* (*derB*) and its ribosome binding site (*derA-derB* 12-bp intergenic region)	This study
pUT18	Vector for B2H, Amp^r	Euromedex, BACTH System Kit Manual
pUT18C	Vector for B2H, Amp^r	Euromedex, BACTH System Kit Manual
pUT18C zip	Control plasmid for B2H, Amp^r	Euromedex, BACTH System Kit Manual
pKT25	Vector for B2H, Kan^r	Euromedex, BACTH System Kit Manual
pKNT25	Vector for B2H, Kan^r	Euromedex, BACTH System Kit Manual
pKT25 zip	Control plasmid for B2H, Kan^r	Euromedex, BACTH System Kit Manual
pUT18C-HK9	*pUT18C* containing histidine kinase *psdS LCABL_16420*	This study
pKT25-HK9	*pKT25* containing histidine kinase *psdS LCABL_16420*	This study
pU-HK9-T18	*pUT18* containing histidine kinase *psdS LCABL_16420*	This study
pKN-HK9-T25	*pKNT25* containing histidine kinase *psdS LCABL_16420*	This study
pUT18C-RR9	*pUT18C* containing response regulator *psdR LCABL_16430*	This study
pKT25-RR9	*pKT25* containing response regulator *psdR LCABL_16430*	This study
pU-RR9-T18	*pUT18* containing response regulator *psdR LCABL_16430*	This study
pKN-RR9-T25	*pKNT25* containing response regulator *psdR LCABL_16430*	This study
pUT18C-Per9	*pUT18C* containing permease *psdB LCABL_16400*	This study
pKT25-Per9	*pKT25* containing permease *psdB LCABL_16400*	This study
pU-Per9-T18	*pUT18* containing permease *psdB LCABL_16400*	This study
pKN-Per9-T25	*pKNT25* containing permease *psdB LCABL_16400*	This study
pUT18C-ATP9	*pUT18C* containing ATPase *psdA LCABL_16410*	This study
pKT25-ATP9	*pKT25* containing ATPase *psdA LCABL_16410*	This study
pU-ATP9-T18	*pUT18* containing ATPase *psdA LCABL_16410*	This study
pKN-ATP9-T25	*pKNT25* containing ATPase *psdA LCABL_16410*	This study
pUT18C-HK12	*pUT18C* containing histidine kinase *apsS LCABL_19610*	This study
pKT25-HK12	*pKT25* containing histidine kinase *apsS LCABL_19610*	This study
pU-HK12-T18	*pUT18* containing histidine kinase *apsS LCABL_19610*	This study
pKN-HK12-T25	*pKNT25* containing histidine kinase *apsS LCABL_19610*	This study
pUT18C-RR12	*pUT18C* containing response regulator *apsS LCABL_19600*	This study
pKT25-RR12	*pKT25* containing response regulator *apsS LCABL_19600*	This study
pU-RR12-T18	*pUT18* containing response regulator *apsS LCABL_19600*	This study
pKN-RR12-T25	pKNT25 containing response regulator *apsS LCABL_19600*	This study
pUT18C-Per12	*pUT18C* containing permease *apsB LCABL_19580*	This study
pKT25-Per12	*pKT25* containing permease *apsB LCABL_19580*	This study
pU-Per12-T18	*pUT18* containing permease *apsB LCABL_19580*	This study
pKN-Per12-T25	*pKNT25* containing permease *apsB LCABL_19580*	This study
pUT18C-ATP12	*pUT18C* containing ATPase *apsA LCABL_19590*	This study
pKT25-ATP12	*pKT25* containing ATPase apsA *LCABL_19590*	This study
pU-ATP12-T18	*pUT18* containing ATPase *apsA LCABL_19590*	This study
pKN-ATP12-T25	*pKNT25* containing ATPase *apsA LCABL_19590*	This study
pUT18C-OrPe	*pUT18C* containing permease *derB LCABL_21670*	This study
pKT25-OrPe	*pKT25* containing permease *derB LCABL_21670*	This study
pU-OrPe-T18	*pUT18* containing permease *derB LCABL_21670*	This study
pKN-OrPe-T25	*pKNT25* containing permease *derB LCABL_21670*	This study
pUT18C-OrATP	*pUT18C* containing ATPase *derB LCABL_21680*	This study
pKT25-OrATP	pKT25 containing ATPase *derB LCABL_21680*	This study
pU-OrATP-T18	*pUT18* containing ATPase *derB LCABL_21680*	This study
pKN-OrATP-T25	*pKNT25* containing ATPase *derB LCABL_21680*	This study

[a]Amp^r, ampicillin resistance; Ery^r, erythromycin resistance; Kan^r, kanamycin resistance.

as previously described (46). Aqueous larval extract from *H. illucens* was prepared as previously described (46) and was considered to be at a concentration of 100% (vol/vol) for the MIC assays.

B. subtilis ATCC 6633 was grown in medium A to induce subtilin production as in Banerjee and Hansen (60). Culture supernatant was collected and was considered to be at a concentration of 100% (vol/vol) for MIC assays.

Antibiotic sensitivity testing. MIC assays were performed in 96-well microtiter plates as previously described (32). Overnight cultures of the strains under study were prepared with antibiotic selection when required, but no antibiotic was added for the MIC assays. The 96-well plates were incubated at 37°C under static conditions in a Synergy NeoalphaB multimode microplate reader (BioTek, Winooski, VT).

TABLE 4 Primers used in this study

Primer name or purpose	Binding site (gene or vector) or amplified product (B2H protein)	Sequence (5′–3′)[a]
Cloning		
RG037	*LCABL_08550*	AGTCAAGCTTGTTCAGATTATTCGCGCACC
RG038	*LCABL_08550*	GACTACTAGTCTGACACTTGATTGCCTTGC
RG047	*LCABL_16400*	**CTATAGGGCGAATTG**GGTACCGCAAGCCTTCAGTATCGCCG
RG048	*LCABL_16400*	**CTCGAGGGGGGGCCC**GGTACCTCAGCCGCGTTTTGATAGCG
RG062	*LCABL_21680*	TTTTCTCGAGTCAGGTTCAGGGAAAACGAC
RG063	*LCABL_21680*	GTGCGACCTAAAGGATCTTTTCTAGACGACGCCCCTTACTTTTG
RG064	Intergenic region *LCABL_21670* and *LCABL_21660*	CAAAAGTAAGGGGCGTCGTCTAGAAAAGATCCTTTAGGTCGCAC
RG065	*LCABL_21660*	AAAAGAATTCCGCCTCAAAAGACTTCATGC
RG220	*LCABL_21670*	AAAAACTAGTTTAGGCTTTTTCCGCTAAGTTCTTATTG
RG221	*LCABL_21670*	AAAAAGATCTGGGGCGTCGTCTATGTTAACG
Cloning checking		
pRV300.fw	pRV300 vector	GTTTTCCCAGTCACGAC
pRV300.rv	pRV300 vector	CAGGAAACAGCTATGAC
pT1NX.fwd	pT1NX vector	TGGATTGGATTAGTTCTTGTGG
pT1NX.rev	pT1NX vector	CTTCTCTGTCGCTATCTGTTG
RG068	LCABL_21660	TATGAAGTCGGCTTCCCGCATG
RG069	LCABL_21680	GTGAATTCGTCGGCATCATG
RG076	LCABL_21680	AACACCCGCATTGAAAGGTG
RG077	LCABL_21660	TCAGCAAAAACGTCACTGGC
LSEI1418R	LCABL_16410	GTCAACATTACTTAAATTAAAAA
qRT-PCR		
lepA-F	*lepA*	CACATTGATCACGGGAAGTC
lepA-R	*lepA*	GTAATGCCACGTTCACGTTC
ileS-F	*ileS*	ACCATTCCGGCTAACTATGG
ileS-R	*ileS*	TCAGGATCTTCGGATTTTCC
pcrA-F	*pcrA*	CGGCCAATAATGTGATTCAG
pcrA-R	*pcrA*	TCATCAGTTTCGCTTTGAGC
pyrG-F	*pyrG*	AATTGCGCTTTTCACTGATG
pyrG-R	*pyrG*	CGAAATGATCGACCACAATC
RG006	*LCABL_19580*	GGGAACGCGCATTCATTGTG
RG007	*LCABL_19580*	TCTCGCGCTGAACAAGATCC
RG008	*LCABL_21670*	TTGCCGGTATTTTGGTCGGG
RG009	*LCABL_21670*	ATGTCCACAATACGGCTGGC
RG019	*LCABL_08550*	TGGTCGAGGTTTTCTTGGGC
RG020	*LCABL_08550*	CCGGTGTATGGGCAACATCC
RG021	*LCABL_24490*	GCCGGATCAGCCAAGACTTG
RG022	*LCABL_24490*	TTAGCATCGGTGTAACGGCG
RG027	*LCABL_19590*	TAGCTTTCAGGTCAACGCGG
RG028	*LCABL_19590*	CTTGGCGTCTCAATCGTTGC
RG029	*LCABL_19600*	GGCAATGAATATGGGCGCTG
RG030	*LCABL_19600*	TAGGTTCGTCGAAGCAAGGC
RG031	*LCABL_21680*	CACCCGCATTGAAAGGTGTC
RG032	*LCABL_21680*	GCAAGGTCGTTTTCCCTGAAC
RG033	*LCABL_16410*	GGACAGGATCTGAGCAACGTC
RG034	*LCABL_16410*	ATTGAAGGTGTCAAGCAAGTCG
RG054	*LCABL_16400*	GTACCGTCCTTTCCCGCATC
RG055	*LCABL_16400*	CCGATGGTAATGATCCCGGC
RG056	*LCABL_16430*	AGCGAGTTACGCAAACACAG
RG057	*LCABL_16430*	CGGCTCCTAAGTTCATCGCC
B2H		
TM1220	pUT18 fwd	AGCTCACTCATTAGGCACCC
TM1221	pUT18 rev	CCGTCGTAGCGGAACTGGCG
TM1222	pUT18C fwd	TCGACGATGGGCTGGGAGCC
TM1223	pUT18C rev	AGCAGACAAGCCCGTCAGGG
TM1224	pKT25 fwd	GGCGGATATCGACATGTTCG
TM1225	pKT25 rev	ATCGGTGCGGGCCTCTTCGC
TM1226	pKT25N fwd	GCTCACTCATTAGGCACCCC
TM1227	pKT25N rev	GGCGGAACATCAATGTGGCG
TM5702	HK9-B2H-XbaI.fw1	AAAATCTAGAGATGATGAAAGCTTATTGCCGCTCG

(Continued on next page)

TABLE 4 (Continued)

Primer name or purpose	Binding site (gene or vector) or amplified product (B2H protein)	Sequence (5′–3′)[a]
TM5703	HK9-B2H-SmaI.rv1	AAAACCCGGGTTACTCCACTTGCCACCGCG
TM5704	HK9-B2H-SmaI.rv2	AAAACCCGGGGCTCCACTTGCCACCGCGTTTG
TM5705	RR9-B2H-XbaI.fw1	AAAATCTAGAGATGGCACAGAAAATTTTTATTGTCGAAG
TM5706	RR9-B2H-SmaI.rv1	AAAACCCGGGTCATGGCTTTGGTCCCTCAC
TM5707	RR9-B2H-SmaI.rv2	AAAACCCGGGGTGGCTTTGGTCCCTCACTTGC
TM5708	ATP9-B2H-XbaI.fw1	AAAATCTAGAGATGTCAACATTACTTAAATTAAAAAATATCGAAAAAAC
TM5709	ATP9-B2H-BamHI.rv1	AAAAGGATCCTCTCATTGTCCATCGCCTGCCTTTG
TM5710	ATP9-B2H-BamHI.rv2	AAAAGGATCCTCTTGTCCATCGCCTGCCTTTG
TM5711	Per9-B2H-XbaI.fw1	AAAATCTAGAGATGAAATTCTACTTTAAGCTCGCTGC
TM5712	Per9-B2H-SmaI.rv1	AAAACCCGGGTTAGCTGCGACTGGTAGCTTGG
TM5713	Per9-B2H-SmaI.rv2	AAAACCCGGGGGCTGCGACTGGTAGCTTGGC
TM6396	HK12-B2H-XbaI.fw1	AAAATCTAGAGATGCGGTTTCGTGATTATTTAAAGG
TM6397	HK12-B2H-SmaI.rv1	AAAACCCGGGTCAGCTGTCTGGATGTGACCTAG
TM6398	RR12-B2H-XbaI.fw1	AAAATCTAGAGGTGTTTAAAATCATGATCGTAGAGG
TM6399	RR12-B2H-SmaI.rv1	AAAACCCGGGCTAAGGAACGATGTAACCTTGTC
TM6400	P12-B2H-XbaI.fw1	AAAATCTAGAGGTGGAGGAGGCCATACCCGTG
TM6401	P12-B2H-SmaI.rv1	AAAACCCGGGCTAATCAATCGCCCAACGGGAAAC
TM6402	A12-B2H-XbaI.fw1	AAAATCTAGAGATGGCAATTCTTGAAGTATCTAACTTGAG
TM6403	A12-B2H-SmaI.rv1	AAAACCCGGGTTAATCAGATGCCACACGGG
TM6404	OrPe-B2H-XbaI.fw1	AAAATCTAGAGATGTTAACGAAACTTGCACTCGG
TM6405	OrPe-B2H-BamHI.rv1	AAAAGGATCCTTAGGCTTTTTCCGCTAAGTTCTTATTG
TM6406	OrA-B2H-XbaI.fw1	AAAATCTAGAGATGGACAAGCAACCTGTCGTAAC
TM6407	OrA-B2H-BamHI.rv1	AAAAGGATCCTTACTTTTGAAATGTGCCGAGTGTG
TM6408	HK12-B2H-SmaI.rv2	AAAACCCGGGGGCTGTCTGGATGTGACCTAGTCTG
TM6409	RR12-B2H-SmaI.rv2	AAAACCCGGGGAGGAACGATGTAACCTTGTCC
TM6410	P12-B2H-SmaI.rv2	AAAACCCGGGGATCAATCGCCCAACGGGAAACAG
TM6411	A12-B2H-SmaI.rv2	AAAACCCGGGGATCAGATGCCACACGGGTATG
TM6412	OrPe-B2H-BamHI.rv2	AAAAGGATCCTCGGCTTTTTCCGCTAAGTTCTTATTG
TM6413	OrA-B2H-BamHI.rv2	AAAAGGATCCTCCTTTTGAAATGTGCCGAGTGTG

[a]Restriction sites are underlined. Sequences highlighted in boldface type are the sequences for the CloneEZ PCR as in Revilla-Guarinos et al. (32).

Growth was monitored by changes in optical density at 595 nm (OD_{595}). For each strain, the MIC at 15 h was defined as the lowest antibiotic concentration where the final OD was at or below the starting OD. All experiments were performed at least in duplicate.

Microscopy. Stationary-phase cell cultures assessed in MIC assays were photographed. Morphology of cultures grown for 24 h in MRS was taken as the reference. Possible morphological changes on bacteria were checked after exposure for 24 h to BR005, BR080, BR081, BR087, BR088, BR090, BR091, BR092, subtilin, and *H. illucens* larval extracts. The cells were observed in an Olympus AX70 microscope with phase contrast at ×40 magnification. Pictures were taken with an Olympus U-TV1XC camera. Pictures were analyzed using the tools implemented in the Olympus cellSens Dimensions 1.14 software and Corel Photo Paint X5.

The average cell length of the bacteria (μm; $n = 200$), the average cell chain length (μm; $n = 40$ cell chains) and the average number of cells per chain ($n = 40$ cell chains) of the stationary-phase cell cultures photographed were determined using the tools implemented in ImageJ 1.52i software (61). Unpaired *t* tests (two-tailed *P* value, 95% confidence intervals) comparing the values of BL23 and the Δ*derB* strain under the reference condition indicated significantly different ($P < 0.05$) means for the cell chain length (*P* value = 0.023) and for the number of cells per chain (*P* value = 0.002). To determine whether the morphological phenotypes of the mutant strain upon exposure to each insect-derived AMP assayed were significantly different from that of the wild type, pairwise two-way analysis of variance (ANOVA) analyses were run with GraphPad Prism 5 software, testing the values of both strains under the reference condition and after each AMP exposure. A difference was considered significant when the analysis estimated *P* values of less than 0.01.

Cytochrome *c* binding assay. Comparison of the whole-cell surface charge of the wild-type strain and Δ*derB* mutant was performed by a cytochrome *c* binding assay as described in Revilla-Guarinos et al. (32). Briefly, cells in the stationary phase at 10^{10} CFU · ml^{-1} were incubated with 150 $\mu g \cdot ml^{-1}$ cytochrome *c* (Sigma) in 20 mM morpholinepropanesulfonic acid (MOPS), (pH 7) for 10 min at room temperature. The mixture was centrifuged twice, and the absorbance of the supernatant (containing unbound cytochrome *c*) was determined at 530 nm. The binding ratio was calculated by comparing the absorbance of each supernatant after incubation with the cells to the absorbance of the cytochrome *c* solution without bacterial cells.

Antimicrobial peptide information and structure predictions. The Antimicrobial Peptide Database (APD) (http://aps.unmc.edu/AP/main.php) (8) was used as a reference for the information listed in Table 1. For structural information, the Protein Data Bank (www.rcsb.org) (62) or UniProt (http://www.uniprot.org/) (63) was used. The structures of plectasin (PDB identifier [ID] 1ZFU [64]), BR080 (sapecin A; PDB ID 1L4V [65]) and BR088 (lucifensin; PDB ID 2LLD [66]) were used. If no structure was available, the

Swiss-Model webpage (https://swissmodel.expasy.org/) was used to generate structural predictions (67–70). The structures of BR081, BR087, BR089, BR090, BR091, and BR092 were modeled by applying the sapecin A structure (PDB ID 1L4V) as the template. Structural comparison was performed with the YASARA View (www.yasara.org) program. Multiple-sequence alignment of the defensins was performed with the CLC Main Workbench 7.7.3 program.

Reverse transcription and quantitative real-time PCR. Samples for RNA isolation were collected as previously described (32). Nisin (22.5 ng · ml^{-1} and subtilin (1% [vol/vol]) were used for the induction assays. Isolation of total RNA from *L. casei* strains, synthesis of cDNA, primer design, and quantitative real-time PCR (qRT-PCR) were carried out as described previously (71). Primers used are listed in Table 4. *lepA*, *ileS*, *pyrG*, and *pcrA* were used as constitutive reference genes (71). Linearity and amplification efficiency for each primer pair were previously determined (32). The relative expression based on the expression ratio between the target genes and reference genes was calculated using the software tool REST (72). Each real-time PCR determination was performed at least six times.

SUPPLEMENTAL MATERIAL

Supplemental material is available online only.

SUPPLEMENTAL FILE 1, PDF file, 0.8 MB.

ACKNOWLEDGMENTS

This work was financially supported by DFG grant MA2837/3-2 (to T.M.) and by funds from the former Spanish Ministry of Science and Innovation and FEDER (grant AGL2010-15679) and the Generalitat Valenciana (grant ACOMP2012/137) (to M.Z.). A.R.-G. thanks the Federation of European Microbiological Societies for research grant FEMS-RG-2014-0067. Q.Z. is financially supported by a stipend from the China Scholarship Council (CSC).

A.M. thanks Herwig Gutzeit (TU Dresden) for his encouragement regarding the *Hermetia illucens* projects, and Bio.S Biogas GmbH (Grimma, Germany), where *Hermetia illucens* cultures were maintained under the supervision of Dennis Hluschi.

We declare no conflicts of interest.

A.R.-G., M.Z., and T.M. conceived the study and planned the experiments. A.R-G. analyzed the data and wrote the manuscript under the supervision of T.M.; M.Z. and S.G. contributed to discussing the results and the final manuscript; A.R.-G. carried out most of the experiments with *L. casei* and designed the B2H constructs; C.A. contributed to the construction of the mutant strains and to the qRT-PCR experiments; Q.Z. performed the B2H cloning and experiments; C.L. performed the structural analysis of defensins and contributed to writing of the manuscript; A.M. prepared *H. illucens* larval extracts; M.R. and A.V. prepared insect-derived AMPs. All authors read the paper and commented on the final manuscript.

REFERENCES

1. Ageitos JM, Sánchez-Pérez A, Calo-Mata P, Villa TG. 2016. Antimicrobial peptides (AMPs): ancient compounds that represent novel weapons in the fight against bacteria. Biochem Pharmacol 133:117–138. https://doi.org/10.1016/j.bcp.2016.09.018.
2. Hancock REW, Chapple DS. 1999. Peptide antibiotics. Antimicrob Agents Chemother 43:1317–1323. https://doi.org/10.1128/AAC.43.6.1317.
3. Draper LA, Cotter PD, Hill C, Ross RP. 2015. Lantibiotic resistance. Microbiol Mol Biol Rev 79:171–191. https://doi.org/10.1128/MMBR.00051-14.
4. Perron GG, Zasloff M, Bell G. 2006. Experimental evolution of resistance to an antimicrobial peptide. Proc Biol Sci 273:251–256. https://doi.org/10.1098/rspb.2005.3301.
5. Brogden KA. 2005. Antimicrobial peptides: pore formers or metabolic inhibitors in bacteria? Nat Rev Microbiol 3:238–250. https://doi.org/10.1038/nrmicro1098.
6. Brötz H, Josten M, Wiedemann I, Schneider U, Götz F, Bierbaum G, Sahl HG. 1998. Role of lipid-bound peptidoglycan precursors in the formation of pores by nisin, epidermin and other lantibiotics. Mol Microbiol 30:317–327. https://doi.org/10.1046/j.1365-2958.1998.01065.x.
7. Oppedijk SF, Martin NI, Breukink E. 2016. Hit 'em where it hurts: the growing and structurally diverse family of peptides that target lipid-II. Biochim Biophys Acta 1858:947–957. https://doi.org/10.1016/j.bbamem.2015.10.024.
8. Wang G, Li X, Wang Z. 2016. APD3: the antimicrobial peptide database as a tool for research and education. Nucleic Acids Res 44:D1087–D1093. https://doi.org/10.1093/nar/gkv1278.
9. McAuliffe O, Ross RP, Hill C. 2001. Lantibiotics: structure, biosynthesis and mode of action. FEMS Microbiol Rev 25:285–308. https://doi.org/10.1111/j.1574-6976.2001.tb00579.x.
10. Dias RDO, Franco OL. 2015. Cysteine-stabilized $\alpha\beta$ defensins: from a common fold to antibacterial activity. Peptides 72:64–72. https://doi.org/10.1016/j.peptides.2015.04.017.
11. Yi HY, Chowdhury M, Huang YD, Yu XQ. 2014. Insect antimicrobial peptides and their applications. Appl Microbiol Biotechnol 98:5807–5822. https://doi.org/10.1007/s00253-014-5792-6.
12. Revilla-Guarinos A, Gebhard S, Mascher T, Zúñiga M. 2014. Defence against antimicrobial peptides: different strategies in *Firmicutes*. Environ Microbiol 16:1225–1237. https://doi.org/10.1111/1462-2920.12400.
13. Neuhaus FC, Baddiley J. 2003. A continuum of anionic charge: structures and functions of D-alanyl-teichoic acids in gram-positive bacteria. Microbiol Mol Biol Rev 67:686–723. https://doi.org/10.1128/mmbr.67.4.686-723.2003.
14. Neuhaus FC, Heaton MP, Debabov DV, Zhang Q. 1996. The *dlt* operon in the biosynthesis of D-alanyl-lipoteichoic acid in *Lactobacillus casei*. Microb Drug Resist 2:77–84. https://doi.org/10.1089/mdr.1996.2.77.
15. Ernst CM, Peschel A. 2011. Broad-spectrum antimicrobial peptide resistance by MprF-mediated aminoacylation and flipping of phospholipids. Mol Microbiol 80:290–299. https://doi.org/10.1111/j.1365-2958.2011.07576.x.

16. Peschel A, Jack RW, Otto M, Collins LV, Staubitz P, Nicholson G, Kalbacher H, Nieuwenhuizen WF, Jung G, Tarkowski A, van Kessel KP, van Strijp JA. 2001. *Staphylococcus aureus* resistance to human defensins and evasion of neutrophil killing via the novel virulence factor MprF is based on modification of membrane lipids with L-lysine. J Exp Med 193:1067–1076. https://doi.org/10.1084/jem.193.9.1067.
17. Gebhard S. 2012. ABC transporters of antimicrobial peptides in *Firmicutes* bacteria—phylogeny, function and regulation. Mol Microbiol 86:1295–1317. https://doi.org/10.1111/mmi.12078.
18. Mascher T, Margulis NG, Wang T, Ye RW, Helmann JD. 2003. Cell wall stress responses in *Bacillus subtilis*: the regulatory network of the bacitracin stimulon. Mol Microbiol 50:1591–1604. https://doi.org/10.1046/j.1365-2958.2003.03786.x.
19. Ohki R, Giyanto Tateno K, Masuyama W, Moriya S, Kobayashi K, Ogasawara N. 2003. The BceRS two-component regulatory system induces expression of the bacitracin transporter, BceAB, in *Bacillus subtilis*. Mol Microbiol 49:1135–1144. https://doi.org/10.1046/j.1365-2958.2003.03653.x.
20. Dintner S, Heermann R, Fang C, Jung K, Gebhard S. 2014. A sensory complex consisting of an ATP-binding cassette transporter and a two-component regulatory system controls bacitracin resistance in *Bacillus subtilis*. J Biol Chem 289:27899–27910. https://doi.org/10.1074/jbc.M114.596221.
21. Dintner S, Staron A, Berchtold E, Petri T, Mascher T, Gebhard S. 2011. Coevolution of ABC transporters and two-component regulatory systems as resistance modules against antimicrobial peptides in *Firmicutes* bacteria. J Bacteriol 193:3851–3862. https://doi.org/10.1128/JB.05175-11.
22. Joseph P, Fichant G, Quentin Y, Denizot F. 2002. Regulatory relationship of two-component and ABC transport systems and clustering of their genes in the *Bacillus/Clostridium* group, suggest a functional link between them. J Mol Microbiol Biotechnol 4:503–513.
23. Kobras CM, Piepenbreier H, Emenegger J, Sim A, Fritz G, Gebhard S. 2019. BceAB-type antibiotic resistance transporters appear to act by target protection of cell wall synthesis. Antimicrob Agents Chemother 64:e02241-19. https://doi.org/10.1128/AAC.02241-19.
24. Piepenbreier H, Sim A, Kobras CM, Radeck J, Mascher T, Gebhard S, Fritz G. 2020. From modules to networks: a systems-level analysis of the bacitracin stress response in *Bacillus subtilis*. mSystems 5:e00687-19. https://doi.org/10.1128/mSystems.00687-19.
25. Fritz G, Dintner S, Treichel NS, Radeck J, Gerland U, Mascher T, Gebhard S. 2015. A new way of sensing: need-based activation of antibiotic resistance by a flux-sensing mechanism. mBio 6:e00975. https://doi.org/10.1128/mBio.00975-15.
26. Koh A, Gibbon MJ, Van der Kamp MW, Pudney CR, Gebhard S. 2020. How to make a dial not a switch: control of histidine kinase conformation by an ABC-transporter facilitates need-based activation of antibiotic resistance. bioRxiv https://doi.org/10.1101/2020.02.28.969956.
27. Gebhard S, Fang C, Shaaly A, Leslie DJ, Weimar MR, Kalamorz F, Carne A, Cook GM. 2014. Identification and characterization of a bacitracin resistance network in *Enterococcus faecalis*. Antimicrob Agents Chemother 58:1425–1433. https://doi.org/10.1128/AAC.02111-13.
28. Gebhard S, Mascher T. 2011. Antimicrobial peptide sensing and detoxification modules: unravelling the regulatory circuitry of *Staphylococcus aureus*. Mol Microbiol 81:581–587. https://doi.org/10.1111/j.1365-2958.2011.07747.x.
29. Staroń A, Finkeisen DE, Mascher T. 2011. Peptide antibiotic sensing and detoxification modules of *Bacillus subtilis*. Antimicrob Agents Chemother 55:515–525. https://doi.org/10.1128/AAC.00352-10.
30. Kallenberg F, Dintner S, Schmitz R, Gebhard S. 2013. Identification of regions important for resistance and signalling within the antimicrobial peptide transporter BceAB of *Bacillus subtilis*. J Bacteriol 195:3287–3297. https://doi.org/10.1128/JB.00419-13.
31. Alcántara C, Revilla-Guarinos A, Zúñiga M. 2011. Influence of two-component signal transduction systems of *Lactobacillus casei* BL23 on tolerance to stress conditions. Appl Environ Microbiol 77:1516–1519. https://doi.org/10.1128/AEM.02176-10.
32. Revilla-Guarinos A, Gebhard S, Alcántara C, Staroń A, Mascher T, Zúñiga M. 2013. Characterization of a regulatory network of peptide antibiotic detoxification modules in *Lactobacillus casei* BL23. Appl Environ Microbiol 79:3160–3170. https://doi.org/10.1128/AEM.00178-13.
33. Revilla-Guarinos A, Alcántara C, Rozès N, Voigt B, Zúñiga M. 2014. Characterization of the response to low pH of *Lactobacillus casei* DRR12, a mutant strain with low D-alanylation activity and sensitivity to low pH. J Appl Microbiol 116:1250–1261. https://doi.org/10.1111/jam.12442.
34. Li M, Lai Y, Villaruz AE, Cha DJ, Sturdevant DE, Otto M. 2007. Gram-positive three-component antimicrobial peptide-sensing system. Proc Natl Acad Sci U S A 104:9469–9474. https://doi.org/10.1073/pnas.0702159104.
35. Heeney DD, Gareau MG, Marco ML. 2018. Intestinal *Lactobacillus* in health and disease, a driver or just along for the ride? Curr Opin Biotechnol 49:140–147. https://doi.org/10.1016/j.copbio.2017.08.004.
36. Dommett R, Zilbauer M, George JT, Bajaj-Elliott M. 2005. Innate immune defence in the human gastrointestinal tract. Mol Immunol 42:903–912. https://doi.org/10.1016/j.molimm.2004.12.004.
37. Hase K, Murakami M, Iimura M, Cole SP, Horibe Y, Ohtake T, Obonyo M, Gallo RL, Eckmann L, Kagnoff MF. 2003. Expression of LL-37 by human gastric epithelial cells as a potential host defense mechanism against *Helicobacter pylori*. Gastroenterology 125:1613–1625. https://doi.org/10.1053/j.gastro.2003.08.028.
38. Pietiäinen M, Gardemeister M, Mecklin M, Leskela S, Sarvas M, Kontinen VP. 2005. Cationic antimicrobial peptides elicit a complex stress response in *Bacillus subtilis* that involves ECF-type sigma factors and two-component signal transduction systems. Microbiology 151:1577–1592. https://doi.org/10.1099/mic.0.27761-0.
39. Müller A, Wolf D, Gutzeit HO. 2017. The black soldier fly, *Hermetia illucens*—a promising source for sustainable production of proteins, lipids and bioactive substances. Z Naturforsch C J Biosci 72:351–363. https://doi.org/10.1515/znc-2017-0030.
40. Schroeder BO, Wu Z, Nuding S, Groscurth S, Marcinowski M, Beisner J, Buchner J, Schaller M, Stange EF, Wehkamp J. 2011. Reduction of disulphide bonds unmasks potent antimicrobial activity of human beta-defensin 1. Nature 469:419–423. https://doi.org/10.1038/nature09674.
41. Zhao C, Wang I, Lehrer RI. 1996. Widespread expression of beta-defensin hBD-1 in human secretory glands and epithelial cells. FEBS Lett 396:319–322. https://doi.org/10.1016/0014-5793(96)01123-4.
42. Matos RC, Leulier F. 2014. Lactobacilli-host mutualism: "learning on the fly. Microb Cell Fact 13(Suppl 1):S6. https://doi.org/10.1186/1475-2859-13-S1-S6.
43. Singh B, Crippen TL, Zheng L, Fields AT, Yu Z, Ma Q, Wood TK, Dowd SE, Flores M, Tomberlin JK, Tarone AM. 2015. A metagenomic assessment of the bacteria associated with *Lucilia sericata* and *Lucilia cuprina* (Diptera: Calliphoridae). Appl Microbiol Biotechnol 99:869–883. https://doi.org/10.1007/s00253-014-6115-7.
44. Rietkötter E, Hoyer D, Mascher T. 2008. Bacitracin sensing in *Bacillus subtilis*. Mol Microbiol 68:768–785. https://doi.org/10.1111/j.1365-2958.2008.06194.x.
45. Peschel A, Otto M, Jack RW, Kalbacher H, Jung G, Götz F. 1999. Inactivation of the *dlt* operon in *Staphylococcus aureus* confers sensitivity to defensins, protegrins, and other antimicrobial peptides. J Biol Chem 274:8405–8410. https://doi.org/10.1074/jbc.274.13.8405.
46. Park S-I, Chang BS, Yoe SM. 2014. Detection of antimicrobial substances from larvae of the black soldier fly, *Hermetia illucens* (Diptera: Stratiomyidae). Entomol Res 44:58–64. https://doi.org/10.1111/1748-5967.12050.
47. Vogel H, Müller A, Heckel DG, Gutzeit H, Vilcinskas A. 2018. Nutritional immunology: diversification and diet-dependent expression of antimicrobial peptides in the black soldier fly *Hermetia illucens*. Dev Comp Immunol 78:141–148. https://doi.org/10.1016/j.dci.2017.09.008.
48. Park SI, Kim JW, Yoe SM. 2015. Purification and characterization of a novel antibacterial peptide from black soldier fly (*Hermetia illucens*) larvae. Dev Comp Immunol 52:98–106. https://doi.org/10.1016/j.dci.2015.04.018.
49. Li Z, Mao R, Teng D, Hao Y, Chen H, Wang X, Wang X, Yang N, Wang J. 2017. Antibacterial and immunomodulatory activities of insect defensins-DLP2 and DLP4 against multidrug-resistant *Staphylococcus aureus*. Sci Rep 7:12124. https://doi.org/10.1038/s41598-017-10839-4.
50. Hammes WP, Hertel C. 2006. The genera *Lactobacillus* and *Carnobacterium*. *In* Dworkin M, Falkow S, Rosenberg E, Schleifer K-H, Stackebrandt E (ed), The prokaryotes, vol 4. Springer-Verlag, New York, NY.
51. Boiocchi F, Porcellato D, Limonta L, Picozzi C, Vigentini I, Locatelli DP, Foschino R. 2017. Insect frass in stored cereal products as a potential source of *Lactobacillus sanfranciscensis* for sourdough ecosystem. J Appl Microbiol 123:944–955. https://doi.org/10.1111/jam.13546.
52. Radeck J, Gebhard S, Orchard PS, Kirchner M, Bauer S, Mascher T, Fritz G. 2016. Anatomy of the bacitracin resistance network in *Bacillus subtilis*. Mol Microbiol 100:607–620. https://doi.org/10.1111/mmi.13336.
53. Kramer NE, van Hijum SA, Knol J, Kok J, Kuipers OP. 2006. Transcriptome analysis reveals mechanisms by which *Lactococcus lactis* acquires nisin

resistance. Antimicrob Agents Chemother 50:1753–1761. https://doi.org/10.1128/AAC.50.5.1753-1761.2006.
54. Randall CP, Gupta A, Utley-Drew B, Lee SY, Morrison-Williams G, O'Neill AJ. 2018. Acquired nisin resistance in *Staphylococcus aureus* involves constitutive activation of an intrinsic peptide antibiotic detoxification module. mSphere 3:e00633-18. https://doi.org/10.1128/mSphereDirect.00633-18.
55. Sambrook J, Fritsch EF, Maniatis T. 1989. Molecular cloning: a laboratory manual. Cold Spring Harbor Laboratory, Cold Spring Harbor, NY.
56. Holo H, Nes IF. 1989. High-frequency transformation, by electroporation, of *Lactococcus lactis subsp. cremoris* grown with glycine in osmotically stabilized media. Appl Environ Microbiol 55:3119–3123. https://doi.org/10.1128/AEM.55.12.3119-3123.1989.
57. Posno M, Leer RJ, van Luijk N, van Giezen MJ, Heuvelmans PT, Lokman BC, Pouwels PH. 1991. Incompatibility of *Lactobacillus* vectors with replicons derived from small cryptic *Lactobacillus* plasmids and segregational instability of the introduced vectors. Appl Environ Microbiol 57:1822–1828. https://doi.org/10.1128/AEM.57.6.1822-1828.1991.
58. Schotte L, Steidler L, Vandekerckhove J, Remaut E. 2000. Secretion of biologically active murine interleukin-10 by *Lactococcus lactis*. Enzyme Microb Technol 27:761–765. https://doi.org/10.1016/s0141-0229(00)00297-0.
59. Karimova G, Pidoux J, Ullmann A, Ladant D. 1998. A bacterial two-hybrid system based on a reconstituted signal transduction pathway. Proc Natl Acad Sci U S A 95:5752–5756. https://doi.org/10.1073/pnas.95.10.5752.
60. Banerjee S, Hansen JN. 1988. Structure and expression of a gene encoding the precursor of subtilin, a small protein antibiotic. J Biol Chem 263:9508–9514.
61. Schindelin J, Arganda-Carreras I, Frise E, Kaynig V, Longair M, Pietzsch T, Preibisch S, Rueden C, Saalfeld S, Schmid B, Tinevez J-Y, White DJ, Hartenstein V, Eliceiri K, Tomancak P, Cardona A. 2012. Fiji: an open-source platform for biological-image analysis. Nat Methods 9:676–682. https://doi.org/10.1038/nmeth.2019.
62. Berman HM, Westbrook J, Feng Z, Gilliland G, Bhat TN, Weissig H, Shindyalov IN, Bourne PE. 2000. The Protein Data Bank. Nucleic Acids Res 28:235–242. https://doi.org/10.1093/nar/28.1.235.
63. The UniProt Consortium. 2017. UniProt: the universal protein knowledgebase. Nucleic Acids Res 45:D158–D169. https://doi.org/10.1093/nar/gkw1099.
64. Mygind PH, Fischer RL, Schnorr KM, Hansen MT, Sönksen CP, Ludvigsen S, Raventos D, Buskov S, Christensen B, De Maria L, Taboureau O, Yaver D, Elvig-Jorgensen SG, Sorensen MV, Christensen BE, Kjaerulff S, Frimodt-Moller N, Lehrer RI, Zasloff M, Kristensen HH. 2005. Plectasin is a peptide antibiotic with therapeutic potential from a saprophytic fungus. Nature 437:975–980. https://doi.org/10.1038/nature04051.
65. Hanzawa H, Shimada I, Kuzuhara T, Komano H, Kohda D, Inagaki F, Natori S, Arata Y. 1990. 1H nuclear magnetic resonance study of the solution conformation of an antibacterial protein, sapecin. FEBS Lett 269:413–420. https://doi.org/10.1016/0014-5793(90)81206-4.
66. Nygaard MK, Andersen AS, Kristensen HH, Krogfelt KA, Fojan P, Wimmer R. 2012. The insect defensin lucifensin from *Lucilia sericata*. J Biomol NMR 52:277–282. https://doi.org/10.1007/s10858-012-9608-7.
67. Biasini M, Bienert S, Waterhouse A, Arnold K, Studer G, Schmidt T, Kiefer F, Cassarino TG, Bertoni M, Bordoli L, Schwede T. 2014. SWISS-MODEL: modelling protein tertiary and quaternary structure using evolutionary information. Nucleic Acids Res 42:W252–W258. https://doi.org/10.1093/nar/gku340.
68. Arnold K, Bordoli L, Kopp J, Schwede T. 2006. The SWISS-MODEL workspace: a web-based environment for protein structure homology modelling. Bioinformatics 22:195–201. https://doi.org/10.1093/bioinformatics/bti770.
69. Guex N, Peitsch MC, Schwede T. 2009. Automated comparative protein structure modeling with SWISS-MODEL and Swiss-PdbViewer: a historical perspective. Electrophoresis 30(Suppl 1):S162–S173. https://doi.org/10.1002/elps.200900140.
70. Kiefer F, Arnold K, Kunzli M, Bordoli L, Schwede T. 2009. The SWISS-MODEL repository and associated resources. Nucleic Acids Res 37:D387–D392. https://doi.org/10.1093/nar/gkn750.
71. Landete JM, García-Haro L, Blasco A, Manzanares P, Berbegal C, Monedero V, Zúñiga M. 2010. Requirement of the *Lactobacillus casei* MaeKR two-component system for L-malic acid utilization via a malic enzyme pathway. Appl Environ Microbiol 76:84–95. https://doi.org/10.1128/AEM.02145-09.
72. Pfaffl MW, Horgan GW, Dempfle L. 2002. Relative expression software tool (REST) for group-wise comparison and statistical analysis of relative expression results in real-time PCR. Nucleic Acids Res 30:e36. https://doi.org/10.1093/nar/30.9.e36.
73. Wang G. 2015. Improved methods for classification, prediction and design of antimicrobial peptides. Methods Mol Biol (Clifton, NJ) 1268:43–66. https://doi.org/10.1007/978-1-4939-2285-7_3.
74. Gasson MJ. 1983. Plasmid complements of *Streptococcus lactis* NCDO 712 and other lactic streptococci after protoplast-induced curing. J Bacteriol 154:1–9. https://doi.org/10.1128/JB.154.1.1-9.1983.
75. Leloup L, Ehrlich SD, Zagorec M, Morel-Deville F. 1997. Single-crossover integration in the *Lactobacillus sake* chromosome and insertional inactivation of the *ptsI* and *lacL* genes. Appl Environ Microbiol 63:2117–2123. https://doi.org/10.1128/AEM.63.6.2117-2123.1997.